Regulation of extracellular ATP of human erythrocytes treated with α-hemolysin. Effects of cell volume, morphology, rheology and hemolysis

M.F. Leal Denis, S.D. Lefevre, C.L. Alvarez, N. Lauri, N. Enrique, D.E. Rinaldi, R. Gonzalez-Lebrero, L.E. Vecchio, M.V. Espelt, P. Stringa, C. Muñoz-Garay, V. Milesi, M.A. Ostuni, V. Herlax, P.J. Schwarzbaum

PII: S0167-4889(19)30009-6
DOI: https://doi.org/10.1016/j.bbamcr.2019.01.018
Reference: BBAMCR 18437

To appear in: *BBA - Molecular Cell Research*

Received date: 2 November 2018
Revised date: 10 January 2019
Accepted date: 30 January 2019

Please cite this article as: M.F.L. Denis, S.D. Lefevre, C.L. Alvarez, et al., Regulation of extracellular ATP of human erythrocytes treated with α-hemolysin. Effects of cell volume, morphology, rheology and hemolysis, BBA - Molecular Cell Research, https://doi.org/10.1016/j.bbamcr.2019.01.018

Regulation of extracellular ATP of human erythrocytes treated with α-hemolysin. Effects of cell volume, morphology, rheology and hemolysis.

M.F. Leal Denis[a,b], S.D. Lefevre[c,d], C.L. Alvarez[a,e], N. Lauri[a,f], N. Enrique[g,h], D.E. Rinaldi[a,i], R. Gonzalez-Lebrero[a,i], L.E. Vecchio[g,h], M.V. Espelt[a,f], P. Stringa[g,j,k], C. Muñoz-Garay[l], V. Milesi[g,h], M.A. Ostuni[c,d], V. Herlax[m,n], P.J. Schwarzbaum[a,f]^.

[a]Universidad de Buenos Aires. Consejo Nacional de Investigaciones Científicas y Técnicas. Instituto de Química y Fisico-Química Biológicas (IQUIFIB) "Prof. Alejandro C. Paladini". Facultad de Farmacia y Bioquímica, Junín 956. Buenos Aires, Argentina.

[b]Universidad de Buenos Aires. Facultad de Farmacia y Bioquímica. Departamento de Química Analítica. Cátedra de Química Química Analítica y Fisicoquímica, Junín 956. Buenos Aires, Argentina.

[c]UMR-S1134, Integrated Biology of Red Blood Cells, INSERM, Université Paris Diderot, Sorbonne Paris Cité, Université de la Réunion, Université des Antilles, F-75015 Paris, France.

[d]Institut National de la Transfusion Sanguine, Laboratoire d'Excellence GR-Ex, F-75015 Paris, France;

[e]Universidad de Buenos Aires. Facultad de Ciencias Exactas y Naturales. Departamento de Biodiversidad y Biología Experimental, Intendente Güiraldes 2160. Buenos Aires, Argentina.

[f]Universidad de Buenos Aires. Facultad de Farmacia y Bioquímica. Departamento de Química Biológica. Cátedra de Química Biológica Superior, Junín 956. Buenos Aires, Argentina.

[g]Universidad Nacional de La Plata. Consejo Nacional de Investigaciones Científicas y Técnicas. Instituto de Estudios Inmunológicos y Fisiopatológicos (IIFP). Facultad de Ciencias Exactas, Calle 47 y 115. La Plata, Argentina.

[h]Universidad Nacional de la Plata. Facultad de Ciencias Exactas. Departamento de Ciencias Biológicas. Cátedra de Fisiología, Calle 47, Casco Urbano. La Plata, Argentina.

[i]Universidad de Buenos Aires. Facultad de Farmacia y Bioquímica. Departamento de Química Biológica. Cátedra de Química Biológica, Junín 956. Buenos Aires, Argentina.

[j]Universidad Favaloro. Consejo Nacional de Investigaciones Científicas y Técnicas. Instituto de Medicina Traslacional, Trasplante y Bioingeniería (IMETTyB), Av. Entre Ríos 495. Buenos Aires, Argentina.

[k]Universidad Nacional de La Plata. Laboratorio de Trasplante de Órganos y Tejidos. Facultad de Ciencias, Calle 60 y 120. La Plata, Argentina.

[l]Instituto de Ciencias Físicas, Universidad Nacional Autónoma de México (UNAM), Av. Universidad s/n. Cuernavaca, México.

[m]Universidad Nacional de La Plata. Consejo Nacional de Investigaciones Científicas y Técnicas. Instituto de Investigaciones Bioquímicas de La Plata (INIBIOLP) "Prof. Dr. Rodolfo R. Brenner". Facultad de Ciencias Médicas, Av. 60 y Av. 120. La Plata, Argentina.

[n]Universidad Nacional de La Plata. Facultad de Ciencias Médicas, Av. 60 y Av. 120. La Plata, Argentina.

^To whom correspondence should be addressed.

Pablo Julio Schwarzbaum, Ph.D., Facultad de Farmacia y Bioquímica, Universidad de Buenos Aires. E-mail: pjs@qb.ffyb.ub.ar, pschwarzbaum@gmail.com

Abstract

Alpha-hemolysin (HlyA) of uropathogenic strains of *Escherichia coli* irreversibly binds to human erythrocytes (RBCs) and triggers activation of ATP release and metabolic changes ultimately leading to hemolysis.

We studied the regulation of extracellular ATP (ATPe) of RBCs exposed to HlyA. Luminometry was used to assess ATP release and ATPe hydrolysis, whereas changes in cell volume and morphology were determined by electrical impedance, ektacytometry and aggregometry.

Exposure of RBCs to HlyA induced a strong increase of [ATPe] (3-36-fold) and hemolysis (1-44-fold), partially compensated by [ATPe] hydrolysis by ectoATPases and intracellular ATPases released by dead cells. Carbenoxolone, a pannexin 1 inhibitor, partially inhibited ATP release (43-67 %).

The un-acylated toxin ProHlyA and the deletion analog HlyAΔ914-936 were unable to induce ATP release or hemolysis.

For HlyA treated RBCs, a data driven mathematical model showed that simultaneous lytic and non-lytic release mainly governed ATPe kinetics, while ATPe hydrolysis became important after prolonged toxin exposure.

HlyA induced a 1.5-fold swelling, while blocking this swelling reduced ATP release by 77 %. Blocking ATPe activation of purinergic P2X receptors reduced swelling by 60-80 %. HlyA-RBCs showed an acute 1.3-2.2-fold increase of $Ca^{2+}i$, increased crenation and externalization of phosphatidylserine. Perfusion of HlyA-RBCs through adhesion platforms showed strong adhesion to activated HMEC cells, followed by rapid detachment. HlyA exposed RBCs exhibited increased sphericity under osmotic stress, reduced elongation under shear stress, and very low aggregation in viscous media.

Overall results showed that HlyA-RBCs displayed activated ATP release, high but weak adhesivity, low deformability and aggregability and high sphericity.

Keywords: hemolysin; ATP-transport; hemolysis; adhesion, aggregation; *E.coli*

Abbreviations: HlyA, α-hemolysin; ATPe, extracellular ATP; ProHlyA, un-acylated protoxin HlyA, HlyAΔ914-936, HlyA-deletion protein; RBCs, erythrocytes; pnx1, pannexin 1; CBX, carbenoxolone; HlyA-RBCs and Pro-RBCs, RBCs exposed to HlyA and ProHlyA respectively; c-RBCs, untreated RBCs; Hb, hemoglobin; Vt, cell volume; Apy, apyrase; $Ca^{2+}i$, intracellular calcium; PS, phosphatidylserine;Vm, membrane potential; SEM, scanning electron microscopy; ATPiv, intravascular ATP.

Introduction

Human erythrocytes (RBCs) can release ATP when exposed to beta-adrenergic stimulation, mechanical deformation, cell adhesion, blood flow turbulence, hypoxia or acidosis (1,2). These treatments mimic several conditions to which RBCs are exposed in the vasculature, e.g. when passing microvascular beds or the contracting skeletal muscle (3–6).

A reduction of ATP release from RBCs has been associated with diseases such as type II diabetes and cystic fibrosis (7–9), while RBCs infection with *Plasmodium falciparum* or exposure to bacterial α-hemolysin correlated with activation of ATP release (10,11).

Intracellular ATP can be released by hemolysis (12) and/or by regulated transport (13). Candidate conduits for regulated ATP release in these cells include several anionic channels (VDAC, maxi anions, volume regulated ion channel and tweety, (13–16), and pore forming proteins like pannexin 1 (pnx1) and P2X7 purinergic receptor (17,18). In addition, α-hemolysin (HlyA) was shown to activate ATP exit of RBCs, presumably by forming pores through which the nucleotide transverses the plasma membrane (10,19).

HlyA is an exotoxin secreted by some pathogenic strains of *E. coli* that causes lysis of several mammalian cells, including RBCs from humans and other mammalian species (20). *In vivo* HlyA has been associated with urinary tract infections and septicemia (21,22). HlyA is synthesized as the protoxin ProHlyA, which is activated by acylation at two internal lysines, Lys-563 and Lys-689. Acylation turns binding of the toxin to the cell membrane irreversible, initiating a series of events leading to hemolysis (23).

The mechanisms enabling ATP release by HlyA are scarcely known, and the putative existence of a receptor for the toxin in erythrocytes remains controversial (24,25). Toxin recognition of RBCs appears to require a short sequence from the C-terminal domain (aminoacid residues 914-936) capable of binding to glycophorins at the RBC surface (26). A deletion mutant lacking these residues lacked hemolytic activity (26), but its effects on ATP release were not tested.

On the other hand, while it has been suggested that during HlyA exposure an early non-lytic ATP release precedes hemolysis (10), parallel dynamic changes in cell volume (Vt) and morphology of RBCs were observed, with unknown consequences on extracellular ATP (ATPe) homeostasis. This is important inasmuch as the extent of ATP release from RBCs, activated by different stimuli, was shown to depend on the capacity of these cells to swell or deform, both in physiological as well as pathological contexts (2,27).

In addition to ATP release, other processes may control ATPe regulation. On the one hand, increased [ATPe], caused by activated ATP exit, can be partly compensated by ectoATPase activity by one or more ectonucleotidases of RBCs and –*in vivo*- of other blood and vascular cells (28). The activities of these enzymes generate extracellular accumulation of ADP and adenosine which, together with ATPe, constitute potent ligands capable of activating purinergic receptors functionally expressed in RBCs (29,30) and endothelial cells (31).

The physiological effects of such ligand-receptor interactions can be manifold. In RBCs, P2X7 activation by ATPe promoted hemolysis (19), a process which should lead to lytic ATP release. In the absence of hemolysis, we found that ATPe activation of P2X2 triggered swelling dependent ATP release (32,33). On the other hand, accumulation of extracellular ADP from ATPe, due to ectonucleotidase activity, led to activation of P2Y13 coupled to inhibition of ATP release (29,33). Thus ATPe regulation depends on the dynamic interaction among ATP release pathways, purinergic receptors signaling and ectonucleotidases.

In this study we characterized how these processes affect ATP regulation of RBCs exposed to HlyA and structural toxin analogs. We made a quantitative assessment of ATPe kinetics, together with a comprehensive description of the main processes controlling HlyA dependent ATP regulation of RBCs. Additionally, we tested the interaction between HlyA and RBCs under different conditions resembling physio-pathological contexts. I.e., ATPe regulation of RBCs was assessed when cells were perfused through a rat mesenteric vascular bed, and video/electron microscopies and rheological techniques were used to assess the capacity of HlyA treated RBCs to change shape, deform or aggregate.

2. Materials and Methods

All reagents in this study were of analytical grade. Bovine serum albumin (BSA), carbenoxolone, digitonin, sucrose, A438079, A740003, human haemoglobin, apyrase (EC 3.6.1.5), firefly luciferase (EC 1.13.12.7), guanidinium hydrochloride, ionomycin, A23175, ATP and dextran 400 were purchased from Sigma (St. Louis, MO, USA). The BCECF-AM, Fluo4-AM, D-luciferin, bis-(1,3-dibutylbarbituric acid)trimethine oxonol ($DiBAC_4(3)$) were purchased from Invitrogen/Molecular Probes Inc. (Eugene, OR, USA). NF110 was purchased from TOCRIS (Bristol, United Kingdom).

2.1 Media used

Tris-Chloride (TC) buffer (in mM) 20 Tris, 150 NaCl, pH 7.4 at 25 °C.

Isosmotic medium (in mM) 137 NaCl, 2.7 KCl, 2.5 Na_2HPO_4, 1.50 KH_2PO_4, 1.32 $CaCl_2$, 1.91 $MgSO_4$, 5 glucose, pH 7.4 at 25 °C, 300 mosM and supplemented with 0.1 % BSA.

Hyperosmotic medium (in mM) 137 NaCl, 2.7 KCl, 4.72 Na_2HPO_4, 1.50 KH_2PO_4, 1.32 $CaCl_2$, 1.91 $MgSO_4$, 5 glucose, 30 mM sucrose, pH 7.4 at 25 °C, 325 mosM and supplemented with 0.1 % BSA.

Krebs Ringer solution (in mM): 130 NaCl, 4.7 KCl, 1.17 Na_2HPO_4, 1.16 $MgSO_4$, 24.0 mM $NaHCO_3$, 2.5 $CaCl_2$, 6 glucose, pH 7.4 at 25 °C.

2.2 Isolation of human erythrocytes

Immediately after blood collection, plasma, platelets and leukocytes were removed by centrifugation (900 x g at 20 °C for 3 min). The supernatant and buffy coat were removed and discarded. Isolated red blood cells (RBCs) were resuspended and washed three times in isosmotic medium. Packed RBCs were resuspended in isosmotic medium to the corresponding final hematocrit.

2.3 Liposomes preparation

Large unilamellar vesicles (LUVs) of 100 nm were made of palmitoyl-oleoyl-phosphatidylcholine:sphingomyelin:cholesterol (POPC:SM:CHO) in a molar ratio of 2:1:1. They were prepared by mixing the appropriate amount of synthetic pure lipids dissolved in chloroform/methanol (2:1, v/v). Samples were dried under a stream of nitrogen and then placed at high vacuum for 2 h in a glass chamber connected to a vacuum pump. Samples were then hydrated in isosmotic medium containing 50 mM ATP, and exposed to 10 rounds of freezing- thawing before extrusion (10 times) through 100 nm filters in a mini extruder (Avestin, Canada). Non-encapsulated ATP was removed by exclusion chromatography (PD-10, GE Healthcare).

2.4 Purification of HlyA, ProHlyA and HlyAΔ916-934

Different *E. coli* overproducing strains were used to produce and release HlyA and mutants. *E. coli* WAM1824 (*E.coli* JM15 strain transformed with pSF4000) produced and release HlyA (34) and *E.coli* WAM 783 (*E.coli* DH1 strain transformed with pSF4000ΔBamHI, in which a portion of the hlyC gene has been deleted) produced the un-acylated inactive protein ProHlyA (35).

Both *E. coli* strains were gently provided by Dr. Welch (University of Wisconsin Medical School, Madison, Wisconsin). *E.coli* BL21 strain transformed with pSU124 (26) produced HlyAΔ914-

936, i.e., a deletion HlyA mutant lacking 914–936 residues. The plasmid was gently given by Dr. Ostolaza (Universidad del País Vasco, Bilbao, Spain).

All cultures were grown over night at 37 °C in Luria–Bertani medium to late log phase (D_{600nm}= 0.9–1.0). The HlyAΔ914-93 producing strain was induced by 0.4 mM IPTG when 0.6 D was reached. Bacteria were then pelleted, and the supernatants concentrated and partially purified by precipitation with 20 % (v/v) cold ethanol at pH 4.5. Pellets containing HlyA, ProHlyA or HlyAΔ914-936 were collected by centrifugation (14,500 x g at 20 °C for 1 h, Sorvall centrifuge rotor SSA 34) and then resuspended in TC buffer supplemented with 6 M guanidinium hydrochloride. SDS-PAGE gels of these preparations showed a main band at 110 kDa corresponding to more than 90 % of the total protein (Suppl. Fig. 1 A). Protein content of each sample was determined by Bradford (36). To evaluate protein functionality, its hemolytic activity was determined as described below. The resulting proteins were stored at −70 °C in guanidinium hydrochloride.

Throughout text, RBCs exposed to HlyA ProHlyA and HlyAΔ914-936 were denoted as HlyA-RBCs Pro-RBCs and HlyAΔ914-936-RBCs, respectively. Untreated RBCs (i.e., controls) were denoted as c-RBCs.

2.5 Hemolytic assays

Two sets of hemolytic assays were carried out. The first assay evaluated the functionality of the HlyA after purification, while the second assay was performed to establish the HlyA concentration used in experiments with RBCs.

To evaluate HlyA functionality, its hemolytic activity was determined by light scattering of a RBCs suspension exposed to increasing concentrations of the toxin. Briefly, 100 µL of HlyA stock solution was serially diluted in isosmotic buffer (0-69 ng/µL) in a 96-well microtiter plate and mixed with 100 µL of RBCs suspension (3 % hematocrit). The plate was then incubated at 37 °C for 30 min and the absorbance at 600 nm measured with a Multimode Detector DTX 880 Beckman Coulter (Suppl. Fig. 1 B).

To establish the concentration of HlyA to be used in experiments, the hemolytic activity was determined by measuring hemoglobin concentration of the supernatants of RBCs suspensions exposed to increasing concentrations of HlyA. Briefly, 100 µL of RBCs suspension (20 % hematocrit) was added to 100 µL of serial 2-fold dilutions of HlyA (0.5-138 ng/µL) in a microtiter plate. The plate was incubated at 37 °C for 5 min, the suspensions were then collected and centrifuged (12600 x g at 20 °C for 30 s) and the hemolysis was quantified as released hemoglobin by measuring absorbance at 405 nm. Results were expressed as percentage of hemolyzed RBCs (% Hemolysis) as function of HlyA concentration (in log scale) (Suppl. Fig. 1 C). Except otherwise stated, an HlyA concentration producing 0.5 % hemolysis after 5 min was used for most experiments (4.5-5 ng/µL). For experiments using ProHlyA and HlyAΔ914-936, a 10-fold higher concentration than that used for HlyA was used.

2.6 ATP measurements

Extracellular ATP (ATPe) and intracelular ATP (ATPi) were measured using firefly luciferase, which catalyzes the oxidation of luciferin in the presence of ATP to produce light (37,38). Because luciferase activity at 37° C is only 10 % of that observed at 20 °C (39), to maintain full luciferase activity, ATP measurements were performed in a cool chamber of a custom-built luminometer acclimated at 20 °C. Under the experimental conditions, assay volume did not

change during the course of the experiment. Two different types of luminometry determinations were performed, *off-line* and *on-line*.

2.6.1 *Off-line* measurements

For *off-line* luminometry determinations, ATPe was measured as previously described (7,8,32,40,41). Briefly, 100 µL of 20 % RBCs suspension were exposed at 37 °C to 100 µL of HlyA in iso- or hyperosmotic media, in the absence and presence of different blockers. Afterwards, 1.5 µL of the suspension was diluted in 45.5 µL of isosmotic medium (final hematocrit 0.32%) to quantify [ATPe] at different times of toxin exposure. Light emission was transformed into ATPe concentration by means of a calibration curve. That is, at the end of each experiment ATP from 2 to 10 µM was sequentially added to the assay medium from a stock solution of pure ATP dissolved in RBC medium. Hemolysis was assessed in paired samples (see method below). The presence of free hemoglobin originated from the hemolysis of RBCs did not interfere with the luminometric signal (not shown). Results were expressed as ATPe in µM.

2.6.2 *On-line* measurements

On-line luminometry measurements were carried out with ATP-loaded liposomes, similarly to experiments with RBCS performed before (33). Briefly, liposomes ($1.7x10^{10}$, $1.7x10^{11}$ or $2.5x10^{11}$) were laid on coverslips mounted in the assay chamber of the luminometer, incubated with 40 µL of luciferin-luciferase mix reaction and exposed to different concentrations of HlyA. Under the experimental conditions, assay volume did not change during the course of the experiment. In separate experiments, liposomes were permeabilized with digitonin (300 µg/mL) to induce full ATP release. Light emission was transformed into ATPe concentration *vs.* time by means of a calibration curve for each experiment, where increasing concentrations of ATP from 0.5 to 10 µM were sequentially added to the assay medium from a stock solution of pure ATP dissolved in RBC medium. Results were expressed as [ATPe] at every time point of a kinetic curve, with [ATPe] expressed as µM (Suppl. Fig. 2). Alternatively, increases in [ATPe] were evaluated at 20 min post stimulus.

Additionaly, *on-line* luminometry measurements were performed to estimate [ATPi] as describe previously (42). Briefly, RBCs ($1.0x10^5$) were laid on coverslips, incubated with 45 µL of luciferine-luciferase mix reaction for 5 min and permeabilized with digitonin (50 µg/mL). Light emission was transformed into ATPe concentration *vs.* time by means of a calibration curve for each experiment, as described above. After considering the total volume occupied by RBCs present in the chamber, and the relative solvent cell volume, intracellular ATP (ATPi) amounted to 2.02 ±0.10 (N=15).

2.7 Hemoglobin measurements

For each sample taken to assess ATPe by *off-line* luminometry, a paired sample was taken to assess hemolysis. Accordingly, paired samples were centrifuged at 12600 x g and 20 °C for 30 sec and the presence of free hemoglobin in the supernatant was determined by light absorption at 405 nm. Results are expressed as percentage of hemolyzed RBCs (% Hemolysis) with respect to the total number of RBCs.

2.8 Intracellular ATPase activity

Intracellular ATPase activity was determined by *off-line* luminometry, following the decrease of exogenous ATP added to a lysate of RBCs. Briefly, $2x10^6$ and $1x10^7$ RBCs were lysed in a medium with 1 mM PMSF and incubated with ATP (1 to 120 µM) at 37 °C. [ATP] was measured in 1.5 µL aliquots by *off-line* luminometry after 5 and 10 min of ATP addition. Recorded light output was transformed into ATPe concentration by means of a calibration curve. To calculate intracellular ATPase activity, linear functions were fitted to experimental data and the parameters of best fit resulting from the regression were used to calculate the initial rates of ATPe extinction (i.e., intracellular ATPase activity). Results were expressed as µM/min.

2.9 Ecto-ATPase activity

EctoATPase activity was determined by *off-line* luminometry, following the decrease of exogenous ATP added to a suspension of intact RBCs. Briefly, 200 µL RBCs suspensions of 10 % hematocrit (containing approx. $2.22x10^8$ cells) were incubated with ATP (2 to 153 µM) at 37 °C. ATPe concentration was measured in 1.5 µL aliquots of the suspension every 2 min for 10 min. Recorded light output was transformed into ATPe concentration by means of a calibration curve. Linear functions were fitted to experimental data and the parameters of best fit were used to calculate initial rates of ATPe extinction, a measure of EctoATPase activity. Paired samples were collected for parallel hemolysis assessment, so as to estimate and subtract ATPe consumption due to intracellular ATPase activity of lysed cells. Results were expressed as µM/min.

2.10 Apyrase activity

Apyrase activity was assessed by on-time luminometry, following the decay of ATP solutions after addition of apyrase. Briefly, 1 µL of ATP solutions ranging from 0.03 to 30 µM were added to 45 µL of luciferin-luciferase mix reaction and ATP kinetics was measured *on-line* as described above. After attaining a stable signal, 1 µL of apyrase (2 to 80 U/mL) was added and luminiscence decay was continuously monitored for 2 min. Recorded light output was transformed into ATPe concentration by means of a calibration curve. Exponential functions were fitted to experimental data and the parameters of best fit were used to calculate the initial rate of ATPe extinction, i.e. Apyrase activity. Results were expressed as µM/min. For apyrase $t_{1/2}$ values were calculated as ln(2)/k, where k is the kinetic coefficient of the exponential function.

2.11 Cell volume measurements

Changes in cell volume were measured using the coulter counting principle with either Scepter 2.0 (Merck Millipore Japan, Tokyo, Japan) or a Casy analyzer (Schärfe System, Reutlingen, Germany).

2.11.1 Cell Scepter measurements

The Scepter cell counter was used to assess volume of RBCs suspensions exposed to HlyA. Briefly, 100 µL of 20 % RBCs suspensions were exposed at 37 °C to 100 µL of HlyA in iso- or hyperosmotic media, in the absence or presence of different blockers. After 5 and 10 min of HlyA exposure, samples were diluted and aspirated using 40 µm tip sensors, according to the manufacturer's recommendation. Cell counts and cell volume distributions were acquired. Histograms were normalized to standard RBCs volume values (43) and cell volume values

(expressed as total volume, Vt) were obtained from the weighted arithmetic mean of each histogram.

2.11.2Casy measurements

Alternatively, cell volume was measured using a Casy cell analyzer. Briefly, 300 µL of 40 % RBCs suspensions were exposed to HlyA in isosmotic media, in the absence and presence of apyrase (10 U/mL). 10 µL of the suspensions were taken at different time of HlyA exposure and diluted 400-fold before measurements. Cell volume values obtained were expressed as total volume (Vt).

2. 12 Endothelial cell culture in biochips and flow adhesion assay

Human micro vascular endothelial cell line 1 (HMEC-1) cells were seeded at 10^7 cells/mL in Vena8 Endothelial+ Biochips (Cellix Ltd, Dublin, Ireland) previously coated with 40 µL of 0.2% gelatin in PBS. Cells were then incubated at 37 °C for 24 h to allow cell attachment and cultured for 48 hs using a Kima pump (Cellix Ltd.). Mediium was changed via a peristaltic pump system every 2 hours with a 300 µL/min flow. Cells were then activated with TNFα (10 ng/mL) at 37 °C for 24 hours and medium was changed every 2 hours. RBCs were washed and resuspended in isosmotic medium supplemented with 0.5% BSA at 2% hematocrit. Adhesion assays were initiated by perfusion of the RBCs at a 0.2 dyn/cm² for 10 min. This was followed by 5-min of washes at 0.5, 1 and 2 dyn/ cm^2. The whole process was controlled using the Exigo pumps and the Cellix software. Images were taken 1 min before wash using the Zeiss AxioObserver microscope, with a 10X objective. Images were acquired using the ZEN software. Adherent RBCs were counted from 6 representative areas.

2.13 Microscopy

Morphology of RBCs was studied by videomicroscopy of viable cells and by Scanning Electron Microscopy (SEM) of glutaraldehide fixed cells.

2.13.1 Videomicrocopy.

RBCs suspensions (1 % hematocrit) were exposed to vehicle, HlyA, ProHlyA or HlyAΔ914-936 at 20 °C. Preparations were immediately mounted on slides and observed by light microscopy (Biotraza LCD XSP-167SP). Images were acquired for 30 min using a charge-coupled device camera at 100X magnification. Control samples were run with non-treated RBCs.

2.13.2 Scanning Electron Microscopy

RBCs were treated with HlyA or ProHlyA for 30 min and then fixed in 2.5% glutaraldehide. Fixed samples were then coated with graphite by thermal evaporation of charcoal (0.150 Torr at 50 Amp for 30 s) using a Desk Carbon Accessory coater (DENTON VACUUM). Coated samples were placed in a holder and observed by SEM (SJEOL model JSM-IT300-LV). Images were acquired with a Secondary Electron Detector at 30 kV, 10-30 spot size and work distance of 10 mm at high vacuum. Control samples were run with non-treated RBCs.

2.14 Deformability

Deformability changes of RBCs treated with HlyA (or analog proteins) were analyzed by ektacytometry using a LoRRca MaxSis equipment (MechatronicsVR, Hoorn, Netherlands), which quantifies the magnitude of cell elongation as a function of applied osmolality, or as a

function of shear stress. The system has been described elsewhere in detail (44). Briefly, a laser beam is directed to RBCs suspended in polyvinylpyrrolidone (PVP), which are subjected to an osmotic gradient or to a gradient of shear stress, and the diffraction pattern produced by the deformed cells is analyzed by a microcomputer. Based upon the geometry of the elliptical diffraction pattern, an elongation index (EI) is calculated as: EI = (L−W)/(L+W), where L and W are the length and width of the diffraction pattern. An increased EI indicates greater cell deformation and hence greater RBC deformability.

When EI was evaluated as a function of medium osmolarity (80-690 mosm/Kg), yielding characteristic osmoscan curves (Fig. 12 A). The assay was carried out using 250 µL aliquots of 44 % RBCs suspensions exposed to HlyA at 37 °C. Samples were taken 2.5 and 3.5 min after treatment. Control samples were run with non-treated RBCs.

From osmoscan curves five parameters were obtained (45): EI min (minimal EI of the curve), O min (osmolality at El min), El max (maximal El), O max (osmolality at El max) and O hyper (osmolality in the hyperosmotic region). The O min directly correlates with the osmolality producing 50 % hemolysis using a standard osmotic resistance test; EI max corresponds to the maximal elongation of the curve; O hyper corresponds to osmolality at 50 % of EI max and reflects the hydration state, increased intracellular viscosity secondary to osmotic water loss and hemoglobin concentration.

When deformability was evaluated as a function of shear stress, a thin layer of RBCs suspended in PVP at 37 °C was placed between two concentric cylinders and shear stress (0.3 – 30 Pascal) was applied. The assay was carried out with 25 µL of 44 % RBCs suspensions exposed to HlyA (or analog proteins) at 37 °C. Samples were taken 2.5 and 3.5 min after treatment. Control samples were run with non-treated RBCs. All measurements were carried out at 37 °C.

Although deformability measurements were run in media without dextran, to compare results of these experiments with those on aggregability (see below), a few experiments were run in the presence of 3 % dextran 400. Both for shear stress curves and osmoscans, results were similar in the absence and presence of this compound (data not shown).

2.15 Aggregability

Aggregation properties of RBCs were determined at 37 °C by laser backscatter *vs*. time, using a LoRRca MaxSis equipment (MechatronicsVR, Hoorn, Netherlands). A syllectogram was created by plotting laser backscattered intensity (Isc) *vs*.time.

RBCs suspensions (40 % hematocrit) were exposed to vehicle (controls), ProHlyA or HlyA for 5 min at 22°C, , in the presence of 3% dextran 400 to promote aggregation. Samples were subjected to high shear for 2 s to dissociate pre-existing RBCs aggregates. Shearing was then stopped abruptly and the changes in Isc were monitored for another 2 min.

2.16 Calcium content

Intracellular calcium content of RBCs was assessed before and after exposure of HlyA or analog proteins.

RBCs suspensions (0.3 % hematocrit) were loaded with 5 µM Fluo4-AM at 37 °C for 60 min, washed and resuspended in isosmotic medium. 100 µL of RBCs suspensions were loaded in 96-well black-walled, clear-bottom plates (Corning, Inc). Real time fluorescence measurements were carried out using a fluorometric plate reader (Synergy HT. Biotek, BioTek Instruments,

Inc., Winooski, VT, USA). The fluorescent signal was recorded in each well simultaneously every 5 s (λ_{exc}: 485 ± 20 nm; $\lambda_{emission}$ 528 ± 20 nm). After 10 min of stable baselines, RBCs were exposed to vehicle or HlyA (or analog proteins) in the absence or presence of different blockers. At the end of the experiment, 5 µM ionomycin was added as positive control. Results were normalized to baseline values and expressed as relative Cytosolic Calcium Content (Ft/F0), i.e., the ratio of fluorescence signal at t (Ft) over fluorescence signal before treatment (F0).

2.17 Assessment of membrane externalization of phosphatidylserine (PS)

The exposure of PS to the outer membrane leaflet of RBCs was measured using lactadherin binding by flow cytometry using a FACS Canto II flow cytometer (BD Biosciences). Briefly, RBCs suspensions (40 % hematocrit) were incubated at 37 °C and exposed to no toxin (control), HlyA or ProHlyA for 2, 3.5, 5 and 10 min. Samples were then centrifuged (10,000 x g for 10 s) and resuspended in isosmotic medium to a 400-fold dilution; 100 µL of this suspension was then incubated with 100 µL of FITC-conjugated lactadherin (1/25 dilution, Cryopep Enterprise, Montpellier, France) for 10 min at room temperature in the dark. Next, samples were diluted 2-fold in isosmotic medium for measurement. Data was analyzed using the FlowJo software (Tree Star). Results were expressed as percentage of positive RBCs and mean fluorescence intensity. In parallel experiments, RBCs were exposed to 10 µM A231875 (a Ca^{2+}i ionophore) as positive controls.

2.18 Membrane Potential (Vm)

The effects of HlyA on Vm of HlyA-treated RBCs were estimated by monitoring changes in fluorescence intensity using $DiBaC_4(3)$ (46) as described previously (47). Briefly, RBCs suspensions were diluted in isosmotic medium with 1 µM $DiBaC_4(3)$ to a final 0.03 % hematocrit. Fluorescence intensities were quantified at 515 nm (λ excitation = 490 nm) every 3 s with continuous stirring at 100 rpm in a PerkinElmer LS-55 spectro fluorometer (PerkinElmer Ltd., Beaconsfield, United Kingdom). RBCs were exposed to HlyA after 5 min of cell stabilization. Values of Vm were expressed as a fluorescence ratio (Ft/F0), where F0 represents the signal of the 5 min baseline and Ft denotes the signal at given time point.

In separated experiments, calibrations of the fluorescence signal were performed. Briefly, RBCs loaded with $DiBaC_4(3)$ were centrifuged at 12000 × g for 30 s and then resuspended at 0.03 % hematocrit in isosmolar solutions with varying K^+ concentrations (1.5 to 150 mM, Table 3). Fluorescence was registered for 5 min and then 2 µM valinomycin was added. Results were expressed as relative fluorescence intensity (Ft/F0), where F0 denotes the signal obtained in the absence of valinomycin and Ft represents the signal at the stationary state after valinomycin addition. All measurements were performed at 37 °C.

2.19 Mean mesenteric arterial bed pressure (MABP)

Adult male Sprague-Dawley rats (250 ± 30 g) were anaesthetized with Isofluorane (5 and 2 % for induction and maintenance, respectively).

The small bowel (jejunum and ileum) with the vascular pedicle (superior mesenteric artery and portal vein) was isolated following a microsurgical procedure previously described (48).

The whole preparation was placed in an organ bath filled with Krebs solution and kept at 37 °C. The superior mesenteric artery and the portal vein were cannulated with polyethylene tubing and perfused with isosmotic medium at 37 °C (1 mL/min) for 10 min in order to eliminate all rat erythrocytes. A pressure transducer (Letica TRI-201) was connected to the mesenteric artery inflow line and changes were measured continuously. The signals from the force transducers were amplified and driven into an analog–digital board (DT16EZ, Data Translation, Marlboro, MA, USA) mounted in a computer. *On-line* recordings and files for later processing were obtained with the software Labtech Notebook Pro (Laboratory Technology, Wilmington, MA, USA). Then the preparation was washed with isosmotic medium and subsequently perfused with HlyA- or ProHlyA-treated RBCs (10% hematocrit) at 37 °C (1 mL/min). Under each condition, the MABP was constantly monitored and samples of fluids leaving from portal vein were taken at 2-min intervals for ATP and Hb assessment.

2.20 Rat mesentery histology

Following perfusion of RBCs suspension under the different treatments (i.e., controls, HlyA and ProHlyA treated RBCs), samples of the rat small intestine were taken for histological examination of the blood vessels. Briefly, samples were fixed in 10 % formaldehyde solution for 72 h, dehydrated in ascending grades of ethyl alcohol (70 %, 80 %, 90 % and 95 %), then cleared in terpinol and embedded in paraffin and sectioned at 6 mm. The sections were deparaffinized in xylene, embedded in descending grades of ethyl alcohol, washed in water and then stained with hematoxylin and eosin.

2.21 Ethics Statement

Human blood was obtained by venipuncture from healthy volunteers the day each study was performed. The study has been approved by the COBIMED (Committee for Bioethics and Investigation, Facultad de Ciencias Médicas, Universidad Nacional de La Plata, protocol 43) and by CEIC (Committee for Ethics on Clinical Investigation, Facultad de Farmacia y Bioquímica, Universidad de Buenos Aires EXP-UBA: 0048676/2017), according to the requirements of the Declaration of Helsinki and the Argentinean legislation concerning Public Health (laws 25326 and 26529). Written informed consent was given by the donors.

Animal handling followed and conformed to the animal welfare guidelines according to NIH (USA) standards. The study has been approved by the Faculty ethical committee for the use of animals in biological research (protocol P04-01-2017).

2.22 Data analysis

Statistical significance was determined using one-way analysis of variance followed by a Turkey–Kramer test of multiple comparisons. A P value < 0.05 was considered significant. Numbers of determinations (n) from independent preparations (N) are indicated.

3. Results

The effects of HlyA and structural mutants proteins on ATPe regulation were first studied on isolated RBCs suspended in isosmotic medium. In addition, to account for responses in a more *in vivo* context, some experiments were carried out using RBCs challenged by osmotic gradients, shear forces, and perfused through adhesion platform or a rat isolated mesentery bed.

3.1 HlyA-dependent ATPe regulation of RBCs

In the absence of hemolysis ATPe kinetics depends on the dynamic balance between non lytic ATP release by protein conduits of viable cells (increasing [ATPe]) and ATPe hydrolysis by one or more ectonucleotidases (decreasing [ATPe]), i.e. ectoATPase activity. In addition, hemolysis induced by HlyA may release ATP and ATPases. These intracellular enzymes, when released in the extracellular space, could hydrolyze ATPe. It follows an assessment of each of these processes potentially affecting ATPe regulation.

3.2 HlyA induced ATP release

ATPe release was evaluated by *off-line* luminometry at 37 °C using a 10 % hematocrit. HlyA concentration was adjusted to result in 0.5 % hemolysis after 5 min of exposure (Suppl. Fig. 1). Paired samples were taken to assess hemolysis by measuring extracellular Hb (see Methods).

RBCs exposure to HlyA produced a non-linear accumulation of ATPe, with [ATPe] amounting to 27.8 ± 8.6 µM after 10 min exposure, i.e., a 36-fold increase over control values (Fig. 1 A). This increase correlated with activation of hemolysis from 0.20 ± 0.03 to 9.02 ± 2.26 % (Fig. 1 A). Prior to calculating lytic and non-lytic ATP release, a characterization of ATPases affecting ATPe regulation was performed.

Fig. 1. Effects of HlyA on [ATPe], ATPe hydrolysis and hemolysis of RBCs.

(A) ***Kinetics of [ATPe] and hemolysis of HlyA-treated RBCs***. RBCs suspensions (10% hematocrit) were exposed to HlyA at 37 °C for 2-10 min and [ATPe] (grey bars, left axis) and hemolysis (white bars, right axis) were quantified. At t=0, RBCs were treated with vehicle in the absence of HlyA. Results are expressed as µM ATPe and as percentage of hemolyzed RBCs (%Hemolysis) with respect to the total number of RBCs. Results are mean values ± S.E.M. (t=0 min, *N*=20, *n*=16; t=2-4 min and 6-8min, *N*=4, *n*=8; t=5 min and 10, *N*=8, *n*=16). **(B)** ***ATPe hydrolysis by EctoATPase and Intracellular ATPase activities***. EctoATPase activity ($ATPase_{EA}$) and ATPase activity of intracellular ATPases ($ATPase_{IA}$) were estimated as a function ATP (µM). Each point of the curves represents the rate of ATP extinction (µM/min). For EctoATPase activity (close triangles), $2.22x10^8$ viable cells were used, while intracellular ATPase activity was performed with hemolyzates from $2x10^6$ cells (white circles) or 10^7 cells (white squares). Dashed lines represent the fitting of linear functions to experimental data. Results are mean values ± S.E.M. **(C)** ***Relative contribution of ATP fluxes to ATPe kinetics of HlyA-treated RBCs***. Experimental data on ATPe kinetics and hemolysis (A), ectoATPase and intracellular ATPase activities (B) were fed into a mathematical algorithm to estimate the relative contribution of these processes to [ATPe] when RBCs were exposed to HlyA for 0-10 min. Details of the mathematical procedure are given in the Suppl. File. $ATPe_L$=ATPe produced by hemolytic release of intracellular ATP; $ATPe_{IA}$= ATPe consumed by intracellular ATPases released by hemolysis; $ATPe_{EA}$=ATPe consumed by EctoATPase activity. $ATPe_{NL}$= ATPe produced by non-lytic release of intracellular ATP, calculated by using the algorithm. *Inset:* Data from main graph during the first 5 min.

Numbers of determinations (*n*) from independent preparations (*N*) are indicated. HlyA concentration was adjusted to result in 0.5% hemolysis after 5 min at 37 °C, value obtained from data of Suppl. Fig.1.

3.3 ATPases

Changes in [ATPe] were detected by *off-line* luminometry. EctoATPase activity was assessed by adding exogenous ATP (2—153 μM) to a suspension of RBCs in the absence of toxin, and following the rate of ATPe decay. Values of initial decay rates for each [ATPe] were used to build a substrate curve. EctoATPase activity *vs.* [ATPe] was approximated by a linear function with slope of the curve (K_{EA}, see Eq. 6 of Suppl. File) amounting to 0.052 min^{-1} (Fig. 1 B).

To assess intracellular ATPase activity, RBCs were lysed and homogenized. Exogenous ATP (1-120 μM) was added to the reaction mixture containing aliquots of homogenate samples in the absence of toxins, and the rate of [ATPe] decay was followed. Repeating this procedure for each [ATP] allowed to build a substrate curve. ATPase activity *vs.* [ATP] was approximated by a linear function with slope of the curve (K_{IA}, see Eq. 7 of S1 File) amounting to 0.014 min^{-1} (Fig.1 B).

Results showed that intracellular ATPase activity increased with the volume of the homogenate -representing the number of dead cells- and with [ATP].

Having experimentally determined ATPe kinetics, ectoATPase activity, and intracellular ATPase activity of HlyA-exposed RBCs (HlyA-RBCs), we built a simple numerical algorithm (see Suppl. File) to calculate the dynamic contribution of each ATP flux to [ATPe] kinetics.

3.4 Modeling ATPe kinetics

When modeling ATPe kinetics, ATP efflux and ATPe hydrolysis were treated as ATP fluxes. Thus, following HlyA exposure, [ATPe] may increase by lytic (J_L, i.e. lytic flux) and non-lytic (J_{NL}, i.e. non-lytic flux) ATP release, and decrease by hydrolysis due to ectoATPase activity (J_{EA}, i.e. ectoATPase flux) or intracellular ATPases of hemolyzed RBCs (J_{IA}, i.e intracellular ATPase flux).

ATPe kinetics was expressed as:

$d[ATPe]/dt = J_{NL}+J_L-J_{EA}-J_{IA}$

This equation was fed with experimental data as follows:

d[ATPe]/dt, J_L, J_{EA} and J_{IA} were estimated by fitting empirical functions to experimental data of Figs. 1 A-B. We then used these functions to calculate the magnitudes of the fluxes, and their contribution to [ATPe], at any time from 0-10 min. A detailed description of the calculations is given in the Suppl. File. The only unknown flux was J_{NL}, whose kinetics was derived using the other fluxes and the values of d[ATPe]/dt.

Following this procedure, results of Figs. 1 A-B could be expressed as in Fig. 1 C, where the relative contribution of each flux to ATPe kinetics can be seen.

ATPe kinetics was dominated by simultaneous lytic and non-lytic release of ATP. ATPe hydrolysis by J_{EA} and J_{IA} was relatively low, although their strength increased with time, thus reducing [ATPe] by 23 % at 10 min post stimulus.

The lytic component (ATP_L) was relevant at all times of toxin exposure, and it amounted to 32 % of total ATPe at 10 min post stimulus, *vs.* 50 % for the contribution of non-lytic ATPe (ATP_{NL}) release to total ATPe.

3.5 Non-lytic HlyA-dependent ATP release

Lytic ATP release did not fully account for the observed increase of [ATPe] in HlyA-RBCs, since a simultaneous non-lytic ATP efflux (J_{NL}) was activated. Both J_L and J_{NL} were relatively low at first, but steeply increased beyond 7 min of toxin exposure.

By considering the intracellular ATP content of RBCs (32) and the number of viable cells at any time, the energetic cost of viable cells to produce J_{NL} was calculated. As shown in Table 1, for

the first 5 min of toxin treatment the contribution of J_{NL} to [ATPe] kinetics required <1 % of intracellular ATP. Thus it did not impose an energetic burden to RBCs. In the late phase of the response (8-10 min), however, the required intracellular ATP steeply increased to approx. 11 %.

Table 1. Time course of ATP_{NL}, and its relationship to intracellular ATP

Time (min)	$ATPe_{NL}$ (µM)	% $ATPe_{NL}/ATP_{intra}$
0	0.16	0.07
2	0.43	0.19
4	1.16	0.51
5	1.92	0.85
6	3.17	1.4
8	8.64	4.04
10	23.58	11.39

ATP_{NL} is shown as ATP_{NL} values (µM), taken from Fig 1 C, or relative (%) to the experimentally determined intracellular ATP content (ATPintra). In the experimental conditions, intracellular ATP of RBCs amounts to 2.05 mM (32).

The mechanisms mediating this flux were studied. RBCs were exposed to HlyA protein analogs differing slightly in structure with HlyA. In addition, the effects of HlyA on ATP loaded liposomes were tested. Finally, RBCs were pre-incubated with carbenoxolone (CBX), a well-known pnx1 inhibitor, prior to HlyA challenge.

3.6 HlyA and protein analogs

To gain insight into structure-function relationships, RBCs were exposed to ProHlyA and HlyAΔ914-936. ProHlyA is the un-acylated precursor of HlyA, known to be hemolytically inactive (49,50), while HlyAΔ914-936 is a HlyA deletion protein lacking a short segment (residues 914–936) known to bind glycophorins on the surface of RBCs membranes (26).

To assess ATP release, RBCs were exposed to these toxin analogs for 5 or 10 min at a concentration ten times that used for HlyA. Results showed a small, but non-significant [ATPe] increase with either compounds (Fig. 2 A). Nevertheless, HlyAΔ914-936 and ProHlyA were functional, in that they induced crenation of RBCs (see section 3.10). Moreover, although HlyA acutely increased $Ca^{2+}i$ (a signal of eryptosis), HlyAΔ914-936 and ProHlyA were unable to induce increases of $Ca^{2+}i$ content (see section 3.10). Thus both fatty acids covalently bound to the toxin, converting ProHlyA into HlyA, and the protein segment responsible for glycophorins binding on RBCs membrane are important structural components of HlyA enabling ATP release.

Fig. 2. ATPe and hemolysis from RBCs exposed to HlyA and protein analogs and ATP release from ATP-loaded liposomes.

(A) ***Effects of HlyA and protein analogs on [ATPe] and hemolysis of RBCs***. RBCs suspensions (10 % hematocrit) were exposed to HlyA, ProHlyA or HlyAΔ914-936 at 37 °C. At 5 and 10 min samples were taken to quantify [ATPe] (grey bars, left axis) and hemolysis (white bars, right axis). Controls were assessed using RBCs suspensions treated with vehicle. Results are expressed as µM ATPe and as percentage of hemolyzed RBCs (% Hemolysis) with respect to the total number of RBCs. Results are mean values ± S.E.M. (*N*=8, *n*=16) (*, significant *vs.* Control; &, significant *vs* mutants; ns, non-significant between each other and Control). **(B)** ***ATP release of ATP-loaded liposomes exposed to HlyA.*** [ATPe]

increments as a function of liposome number for different HlyA concentrations. Liposomes ($1.7x10^{10}$, $1.7x10^{11}$ and $2.5x10^{11}$) were exposed to 11 ng/µL (white bars) and 22 ng/µL (grey bars) of HlyA and ATP release was measured by *on-line* luminometry. Results are expressed as µM ATPe and are mean values ± S.E.M. (*N*=2, *n*=4) of [ATPe] at 20 min post stimulus. Results were obtained from similar ATPe kinetics curves shown in Suppl. Fig. 2 B. **(C)** ***Effects of carbenoxolone on HlyA-induced ATP release and hemolysis.*** RBCs suspensions (10 % hematocrit) were pre-incubated for 10 min with or without 100 µM carbenoxolone (CBX), followed by HlyA addition. At 5 and 10 min samples were taken to quantify [ATPe] (grey bars, left axis) and hemolysis (white bars, right axis). Controls were assessed using RBCs suspensions treated with vehicle. Results are expressed in µM ATPe and as percentage of hemolyzed RBCs (% Hemolysis). Results are mean values ± S.E.M. (*N*=4, *n*=8) (*, significant *vs.* Control; &, significant *vs.* CBX treatment).
Numbers of determinations (*n*) from independent preparations (*N*) are indicated. HlyA concentration was adjusted as in Fig. 1. Concentrations of ProHlyA or HlyAΔ914-936 were 10 times the concentration used for HlyA. P< 0.05 was considered significantly different.

3.7 Liposomes

It was previously argued that HlyA *per se* was able to oligomerize and form a pore capable of releasing ATP, so that no endogenous ATP conduit would be needed to explain non-lytic ATP release from RBCs (10).

Based on this hypothesis, we decided to test HlyA dependent ATP release by *on-line* luminometry on liposomes made of PC:SM:Cho (2:1:1), a lipid composition similar to that of the external monolayer of RBCs (51). Liposomes were loaded with 50 mM ATP. To compare results with those using RBCs, extravesicular ATP was denoted as ATPe.

In the absence of HlyA, basal ATPe remained constant at 0.47 µM, showing no ATP leak. Addition of 300 µg/mL digitonin to disrupt liposomes, on the other hand, led to a strong increase of [ATPe] (Suppl. Fig. 2 A).

Exposure to HlyA induced an acute, 1.3-fold increase of [ATPe] (Suppl. Fig. 2 B). ATPe release correlated directly –but non-linearly- with liposome number and HlyA concentration (Fig.2 B). However, to make ATPe detectable relatively high HlyA concentrations (2-5-fold higher than that used with RBCs) and a high intravesicular [ATP] (24-fold higher than intracellular [ATP] of RBCs) had to be used. To compare HlyA induced ATP efflux in liposomes *vs* RBCs, maximal values of [ATPe] increase (at 10 min post-stimulus for RBCs, Fig. 1 A and at 20 min post-stimulus for liposomes, Fig.2 B) were normalized per surface area. Results showed that normalized efflux ($\mu M/\mu m^2$) amounted to $8.50x10^{-10}$ (RBCs) and $9.55x10^{-11}$ (liposomes). I.e., RBCs exhibited a 9-fold higher ATP release, even when –as mentioned above- liposomes contained a much higher intracellular ATP concentration and were exposed to a higher HlyA concentration.

3.8 Effect of carbenoxolone (CBX)

The small increase of [ATPe] induced by exposing liposomes to HlyA suggest that the toxin *per se* is not mediating most of ATP efflux of RBCs. Thus, we investigated whether HlyA induced ATP release of RBCs can be inhibited by CBX, an inhibitor of the ATP conduit pnx1. Accordingly, RBCs were pre-incubated with 100 µM CBX and [ATPe] was determined at 5 and 10 min post-stimulus. Results showed that CBX + HlyA reduced 43-67 % of [ATPe] increase and 43-61 % of hemolysis (Fig. 2 C) induced by HlyA alone.

By using the mathematical algorithm (see Modeling ATPe kinetics above and Suppl. File), the influence of CBX on both the lytic and non-lytic fluxes on ATPe kinetics could be calculated, showing that CBX inhibited both fluxes (Suppl. Fig. 3).

3.9 Interaction between cell volume and [ATPe]

Our previous accounts have shown that [ATPe] and Vt can be mutually regulated in RBCs exposed to amphipatic peptides (33,52). Thus, a series of experiments were conducted to study the relationship between these two variables in HlyA-RBCs.

Results of Fig. 3 A showed the kinetics of Vt challenged by HlyA. Vt was measured by the Coulter Counter principle. Cells very slightly shrunk during the first min post stimulus, followed by continuous swelling up to 40 % of initial control values.

Fig. 3. Effect of HlyA on RBCs volume (Vt). ATPase activity of Apyrase

(A) Time course of Vt of HlyA-exposed RBCs. RBCs suspensions (40 % hematocrit) were pre-incubated for 10 min with or without 10 U/mL of apyrase (Apy) prior to HlyA exposure. Inset: Data from main graph during the first 2.5 min post stimulus. Results are mean values ± S.E.M. (*N*=1, *n*=3). **(B)** ***Volume of HlyA-exposed RBCs***. RBCs suspensions (10 % hematocrit) were pre-incubated at 37 °C for 10 min with or without 10 U/mL Apy, followed by HlyA exposure for 5 and 10 min. Control values refer to RBCs exposed to vehicle. Results are mean values ± S.E.M. (Control, *N*=13, *n*=20; HlyA, *N*=9, *n*= 15; HlyA-Apy, *N*=5, *n*=8). **(C-D)** ***Kinetics of ATP hydrolysis by Apyrase***. The rate of ATP hydrolysis by apyrase (5-20 U/mL) was determined by following the decay of [ATP] 3 µM **(C)** and 30 µM **(D)** by *on-line* luminometry. Results are mean values (*N*=1, *n*=2). The continuous lines represent fittings of exponential functions to experimental data.

Numbers of determinations (*n*) from independent preparations (*N*) are indicated. HlyA concentration was adjusted as in Fig. 1.

Shape dynamics assessed by optical microscopy showed morphological transitions from birefringent discocyte (i.e., normal shape of control RBCs) to echinocyte (spiculated shape) to spherocyte (nearly spherical) (see section 3.10).

Pre-incubation with excess apyrase (10 U/ml), a well-known ATPe scavenger (53), did not change Vt kinetics (Fig. 3 A), thus suggesting that ATPe was not affecting Vt. This was unexpected since we observed before that ATPe can activate RBCs swelling (33). We then focused on the late swelling phase of the response to HlyA, analyzing average values of Vt taken from volume distribution profiles (Vt histograms, see Suppl. Fig. 4 A).

As expected from Vt kinetics (Fig. 3 A), HlyA induced a 46 % and 60 % Vt increase after 5 and 10 min of toxin exposure, respectively (Fig. 3 B), while in ProHlyA treated RBCs (Pro-RBCs)and non-treated RBCs (c-RBCs) no swelling could be detected (Suppl. Fig. 4 B).

As previously observed, pre-incubation with apyrase did not alter swelling of HlyA-RBCs (Fig. 3 B). Thus, either [ATPe] had no effect on Vt increase, or apyrase was not efficiently removing ATPe under the experimental conditions. We thus used *on-line* luminometry to assess the capacity of apyrase to consume exogenous ATP in the absence of RBCs. Using 0.03-30 µM ATP (covering the range of endogenous [ATPe] observed in Fig. 1), apyrase dose-dependently (5-80 U/mL) decreased [ATPe], with $t_{1/2}$ ranging from 0.01-0.31 min (Fig. 3 C-D and Suppl. Fig. 5).Results implied that ATPe removal by the enzyme was not instantaneous, so that substantial ATPe can still be present when using apyrase in RBCs suspensions treated with HlyA. Thus, as an alternative to removing ATPe, we blocked the effect of the nucleotide on specific purinergic receptors. In particular, we hypothesize that changes in Vt could be controlled by P2X receptor activation by ATPe. In RBCs functional P2X2 and P2X7 subtypes were reported (54,55).

Accordingly, cells were incubated with 600 nM A438079 and 200 nM A740003 (two P2X7 blockers) or 10 µM NF110 (a blocker of P2X1-3) before toxin addition. Results showed the three treatments led to a 52 % (5 min post stimulus)-73 % (10 min post stimulus) reduction of

[ATPe] (Fig. 4 A and B, respectively), and a 53 % (5 min post stimulus)-66 % (10 min post stimulus) reduction of hemolysis (Fig. 4 C and D, respectively) when compared with the effects of the toxin alone.

Fig. 4. Effect of P2X receptors on [ATPe], cell volume and hemolysis of HlyA-exposed RBCs
RBCs suspensions (10 % hematocrit) were used to measure [ATPe] (grey bars) and hemolysis (white bars) at 5 min **(A)** and 10 min post stimulus **(B)**. Cell volume (Vt) was measured in separate samples **(C)**. Before HlyA addition (for 5 or 10 min), RBCs suspensions were pre-incubated for 10 min in the absence (controls) or presence of the following P2X antagonists: 200 nM A740003 (P2X7), 600 nM 438079 (P2X7), 10 µM NF110 (P2X1-2). For hemolysis experiments at 5min HlyA exposure, additional treatments were used, i.e, RBCs were pre-incubated with [10 µM NF110 + 200 nM A740003] or [100 µM CBX + 10 µM NF110 + 200 nM A740003].
A-B: Results are mean values ± S.E.M. (*N*=4, *n*=8). (*, significant *vs*. Control; &, significant *vs*. inhibitors). **C**: Results are mean values ± S.E.M. (Control, *N*=13, *n*=20; HlyA, *N*=9, *n*=15; Inhibitors, *N*=5, *n*=8). (*, significant *vs*. Control; &, significant *vs*. HlyA). Numbers of determinations (*n*) from independent preparations (*N*) are indicated. HlyA concentration was adjusted as in Fig. 1*P*< 0.05 was considered significantly different.

Co-incubation with 10 µM NF110 + 200 nM A740003 or 100 µM CBX + 10 µM NF110 + 200 nM A740003 did not reduce hemolysis beyond reductions obtained with the inhibitors applied separately (Fig. 4 C).
Since inhibition of HlyA dependent [ATPe] increase was similar for A438079 and A740003, and was already observed after 5 min, we tested the effects of A438079 and NF110 on Vt folllowing 5 min exposure to the toxin. It can be seen that NF110 significantly reduced 80 % of the swelling response caused by HlyA, while A438079 produced a similar reduction trend, although results were not significant (Fig. 4 E).
As a final test for the reciprocal regulation of swelling on ATP release, RBCs were exposed to HlyA dissolved in a slight hyperosmotic medium (Hyper-HlyA). During toxin exposure, final medium osmolarity was 10 % over isosmotic values (i.e., 330 mOsm). As observed in Fig. 5 A, swelling was reduced by 70-96 % in Hyper-HlyA, as compared to HlyA under isosmotic conditions. Hyper-HlyA also decreased ATPe release and hemolysis of RBCs (Fig 5 B-C).

Fig. 5. Effect of hyperomoslarity on cell volume, ATPe and hemolysis of HlyA-exposed RBCs
RBCs suspensions (10 % hematocrit) were used to measure [ATPe] (grey bars) and hemolysis (white bars) **(A)**. Cell volume (Vt) was measured in separate samples **(B)**. Cells were exposed to HlyA dissolved in isosmotic medium (300 mOsm) or hyperosmotic medium (330 mOsm) at 37 °C, for 5 and 10 min. Control experiments were run in isosmotic medium in the absence of HlyA. Results are mean values ± S.E.M. (**A**: *N*= 4, *n*= 8; **B**: Control, *N*=13, *n*=20; HlyA, *N*=9, *n*=15; Hyper, *N*=4, *n*=5) (*, significant *vs.* Control; &, significant *vs*. hyperosmotic treatment).
Numbers of determinations (*n*) from independent preparations (*N*) are indicated. HlyA concentration was adjusted as in Fig. 1.*P*< 0.05 was considered significantly different.

3.10 Calcium content, cell shape, PS exposure and membrane potential

To explain mechanisms allowing the observed changes in Vt, ATPe and hemolysis, additional parameters were monitored.
Shrinking was postulated to be triggered by calcium increase, and this should correlate with crenation and PS exposure. The biphasic Vt response, on the other hand, could be due to changes in the net flux of osmolyte ions, in which case changes in the membrane potential (Vm) of the RBCs would be expected.

Accordingly, under HlyA, our results showed an acute increase of Ca^{2+}i concentration (1.3-2.2-fold; Fig. 6 A-C), which could not be blocked by NF110 or A74003 (Fig. 6 B), increased crenation followed by swelling (Fig. 7 B-C), and irreversible PS externalization (Fig. 6 D and Table 2), which are typical features of eriptosis (56).

Fig. 6. Effects of HlyA and protein analogs on calcium content and phosphatidylserine (PS) externalization.
(A-B) ***Cytosolic Calcium Content***. RBCs suspensions (0.3 % hematocrit) were loaded with Fluo4-AM and exposed to ProHlyA or HlyA **(A)**; additionally, before HlyA exposure RBCs suspensions were pre-incubated for 10 min with the following P2X antagonists: 200 nM A740003 (P2X7), 10 µM NF110 (P2X1-2) or 10 µM NF110 + 200 nM A740003. **(B)**. Calcium content was measured after exposure to HlyA or ProHlyA. Ionomycin was used as positive control. Controls were assessed with vehicle.. **(C)** ***Kinetics of calcium content of HlyA-RBCs***. RBCs suspensions (0.3 %) were loaded with Fluo4-AM and exposed to HlyA. Time changes in fluorescence intensity were recorded every 5 s for 10 min. Results are mean values ± S.E.M. (**A-B**: Control, *N*= 8, *n*= 20; ProHlyA, *N*=8, *n*=13; HlyAΔ914-936, *N*=8, *n*=13; HlyA, *N*=8, *n*=46. **C**: *N*=3, *n*=12; NF110, N=4, n=8; A740003, N=4, n=8; NF110+A740003, N=4, n=8) (*, significant *vs.* Control; &, significant *vs.* ProHlyA and HlyAΔ914-936). **(D)** ***Phosphatidylserine (PS) exposure as function of time for HlyA-treated RBCs***. RBCs suspensions (10 % hematocrit) were incubated at 37 °C and exposed to HlyA for 2-10 min. PS exposure was expressed as percentage of positive control and are means values ± S.E.M. (*N*=4, *n*=5). Control values refer to RBCs exposed to vehicle.
Numbers of determinations (*n*) from independent preparations (*N*) are indicated. P< 0.05 was considered significantly different.

Table 2. Values of phosphatidylserine exposure after different treatments.

Control	ProHlyA	HlyA	A23175
0.56 ± 0.09	0.61 ± 0.05	28.04 ± 0.95	93.60 ± 1.77

RBCs were treated with ProHlyA, HlyA or ionophore A23187 (positive control). Results were obtained after incubation RBCs for 10 min under the different conditions. Results are expressed as percentage of positive controls and are means values ± S.E.M. (*N*= 4, *n*=5). Numbers of determinations (*n*) from independent preparations (*N*) are indicated.

Moreover, the membrane potential (Vm) showed an acute hyperpolarization followed by depolarization (Fig. 8 A-B and Table 3), with roughly similar kinetics to that observed for Vt (Fig. 3 and correlation plot of Fig. 8 C).

Fig. 7. Effects of HlyA and protein analogs on RBCs morphology
(A-D) ***Live cell imaging***. Light microscopy images of RBCs suspensions exposed to vehicle **(A)**, HlyA (0.011 and 0.132 ng/µL; **B-C**), ProHlyA (1.32 ng/µL; **D**) or HlyAΔ914-936 (1.32 ng/µL; **E**) at 20 °C.. **(F-H)** ***SEM micrographs***. RBCs were treated with vehicle **(F)**, HlyA **(G)** or ProHlyA **(H)** for 30 min at 20 °C. Samples were fixed in 2.5% glutaraldehyde and coated with graphite. Images were acquired with a Secondary Electron Detector at 30 kV and high vacuum. (**F (a)** scale =20 µm, **(b)** scale = 5 µm; **G (a-b)** scale = 5 µm, different field; **H (a)** scale = 10 µm, **(b)** scale = 2 µm).

When RBCs were exposed to ProHlyA or the deletion protein HlyAΔ914-936, only crenation was observed (Fig. 7 D-E) with no changes in Ca^{2+}i concentration (Fig. 6 B). Moreover, ProHlyA produced no PS externalization (Fig. 6 D and Table 2), although changes in morphology could be verified at higher spatial resolution using SEM. That is, exposure of RBCs to ProHlyA induced the formation of echinocytes (Fig. 7 H), with no hemolysis. On the other hand, HlyA treated RBCs exhibited different morphological changes, where echinocytes and spherocytes could be observed, together with hemolyzed cells (Fig. 7 G).

Fig. 8. Membrane potential (Vm) of HlyA-exposed RBCs

RBCs suspensions were loaded at 37 °C with $DiBaC_4(3)$ and the effects of HlyA on Vm were tested. Results are expressed as florescence relative to basal values (untreated RBCs): Ft/F0. **(A)** ***Kinetics of Vm RBCs exposed to HlyA***.. From 0-5 min, relative basal Vm time course was measured. At 5 min RBCs were exposed to HlyA (*N*=3, *n*=5), and Vm was recorded. The arrow indicates addition of HlyA. **(B)** ***Relative Fluorescence Intensity of $DiBaC_4(3)$ as function of K^+ concentration ($[K^+]$)***. $DiBaC_4(3)$ loaded RBCs were exposed to isosmolar solutions with increased $[K^+]$ in the presence of valinomycin. **(C)** ***Correlation between Vt and Vm***. Data from A was plotted as Vm against values of Vt from Fig. 3 A at different times of HlyA exposure. Numbers of determinations (*n*) from independent preparations (*N*) are indicated.

Table 3. Values of K^+ concentration used in Fig 8 B

$[K^+]$ (mM)
150
137
90
60
30
20
12
1.5

3.11 Adhesion

HlyA-induced PS externalization, as observed in Fig. 6 D, can lead *in vivo* to adhesion of RBCs to vascular endothelial cells (VECs). Thus we tested whether HlyA was able to induce RBCs adhesion to VECs. RBCs suspensions were perfused under controlled flow in adhesion platforms coated with HMEC cells. Fluid flow was initially low (0.2 dyn/cm^2) to allow adhesion, and then increased in 5 min steps to 0.5, 1 and 2 dyn/cm^2 to induce detachment. Irrespective of the treatment (control, ProHlyA or HlyA), adhesion was higher at low flow (0.2 dyn/cm^2), and decreased steadily with flow increments. As seen in Fig. 9 B and Table 4, in HlyA-RBCs adhesion to VECs was strongly increased, as opposed to c- and Pro-RBCs (Fig 9. A and C). However, adhesive forces were weak, as increments in flow induced a high detachment (Fig. 9, panels from left to right).

Fig. 9. Effect of HlyA on RBCs adhesion to endothelial vascular cells

Representative images of RBCs adhesion to HMEC. RBCs suspensions (2 % hematocrit) treated with vehicle **(A)**, HlyA **(B)** or ProHlyA **(C)** were perfused under controlled flow through adhesion platforms coated with HMEC cells. Fluid flow was initially low (0.2 dyn/cm^2) to allow adhesion, and then increased in 5 min steps to 0.5, 1 and 2 dyn/cm^2 to induce detachment. Red arrows indicate adhered RBCs.

Table 4. Number of adhered RBCs to HMEC cells

Control	ProHlyA	HlyA
10 ± 3	5 ± 2	1506 ± 740

Control refers to RBCs-treatment with vehicle. Results are mean values ± S.E.M. (*N*=2, *n*=3). Numbers of determinations (*n*) from independent preparations (*N*) are indicated.

3.12 ATP release of RBCs in a rat mesentery model

HlyA-RBCs exhibited enhanced ATP release by lytic and non-lytic processes. Here, we wondered whether this response is reproduced in a more *in vivo* environment, i.e., when HlyA-

RBCs are continuously perfused through a rat mesenteric vascular bed. This is a heterologous organ system where the entire vascular pedicle and the small intestine remain intact (57).
Mean mesenteric arterial bed pressure (MABP, estimated as pressure in mmHg) was continuously recorded, and intravascular levels of ATP (ATPiv) and free Hb (to estimate lytic ATP release) were measured at discrete times in perfusate samples that leave the arterial bed through the portal vein.
Suppl. Fig. 6 A showed a picture of the model system where the superior mesenteric artery and the portal vein were cannulated for vascular perfusion. Details on the setup are given in Methods. Krebs Ringer solution at 37 °C was perfused at 1 mL/min. After MABP stability, 10 % RBCs suspensions were perfused at the same rate, and MABP was constantly monitored.
As a control for the functional integrity of the smooth muscle cells and the endothelium of the arterial bed, we observed that 10 µM noradrenaline strongly increased MABP due to smooth muscle contraction, while with 20 µM acetylcholine a significant decrease was observed, suggesting a functional endothelium (Suppl. Fig. 6 B); basal values of MABP were obtained when buffer perfusion washed out these compounds.

In separate experiments, the mesentery was perfused with assay media containing ProHlyA or HlyA, in the absence or presence of RBCs, and ATPiv and MABP were measured.
ATPiv was 0.13 ± 0.08 µM with isosmotic medium perfusion, and 0.29 ± 0.14 µM in the presence of RBCs (Fig. 10 A). Perfusion of free HlyA or ProHlyA in the absence of RBCs produced minor changes on ATPiv (0.31 ± 0.11) (Fig. 10 B) while perfusion of ProHlyA plus RBCs further increased ATPiv to 1.19 ± 0.42 µM, with hemolysis amounting to 0.57 ± 0.38 % after 10 min of perfusion (Fig. 10 C). However, when HlyA and RBCs were co-perfused, ATPiv increased from 2.01 ± 0.47 µM at t=1-2 min, to 27.28 ± 7.26 µM at t=9-10min, and hemolysis increased from 4 to 33 % (Fig. 10 D). Parallel determinations of ATPiv and Hb allowed us to estimate the relative contribution of lytic and non-lytic mechanisms of RBCs ATP release when RBCs were flowing inside the arterial bed. As seen in Fig. 10 D, the non-lytic component of ATP release was the major component explaining ATPiv.

Fig. 10. ATP release of RBCs in a rat mesenteric vascular bed and its effect on vascular pressure
Vehicle (buffer) or RBCs suspensions (10 % hematocrit) were perfused through a rat mesentery preparation. Mean mesenteric arterial bed pressure (MABP) was recorded and samples of the perfusates were collected at different times (T1-T5) for assessment of ATP. The latter was denoted as intravascular ATP (ATPiv). **(A)** Perfusion of vehicle or control RBCs suspensions (c-RBCs). **(**B**)** Perfusion of either ProHlyA or HlyA dissolved in buffer, in the absence of RBCs. **(C-D)** Perfusion of RBCs suspension in the presence of either ProHlyA (ProHlyA-RBCs, **C**) or HlyA (HlyA-RBCs, **D**). Samples of the perfusates were collected for assessment of hemoglobin and ATP. Hemoglobin concentration was used to estimate lytic ATP (ATP_L). The difference between [ATPiv] and [ATP_L] was calculated and denoted as non-lytic ATP (ATP_{NL}). A stacked graph was built to show the contribution of lytic and non-lytic ATP release from RBCs to [ATPiv]. **(E)** ***Effect of HlyA-treated RBCs on MABP****.* Assessment of MABP, estimated as Force in mmHg was continuously recorded.
A-D: Results are mean values ± S.E.M. (A, C and D: *N*=2; B: *N*=3). **E**: Results are mean values ± S.E.M. of the highest values registered for each treatment. (*N*=9, c-RBCs; *N*=6, HlyA-RBCs; *N*=3, HlyA-RBCs) (*, significant *vs.* c-RBCs and Pro-RBCs).
Numbers of independent preparations (*N*) are indicated. Concentration of ProHlyA was 10 times the value for HlyA. P< 0.05 was considered significantly different.

On the other hand, in RBCs and Pro-RBCs, MABP values were 18.14 ± 3.32 and 17.32 ± 5.22 mmHg respectively, but when RBCs were perfused plus HlyA, the pressure increased 2-fold

(38.3 ± 7.8 mmHg) compared to RBCs alone (Fig. 10 E), suggesting and additional contractile effect induced by HlyA. Thus, we tested in separate experiments the effect of Hb and exogenous ATP to evaluate their separate effects on vessel contraction. Results showed that high Hb (>10 µM) can induce vasoconstriction, while exogenous ATP did not significantly affect MABP (Suppl. Fig. 6 C-D).

In experiments using RBCs in the absence and presence of HlyA, tissue samples were taken to evaluate the morphology of RBCs inside the vascular system. Tissue sections were stained with hematoxylin-eosine (58) and observed by light microscopy. In the absence of toxins, RBCs of arteries, capillaries and veins showed a conserved morphology. With HlyA, on the other hand, RBCs showed altered morphology and apparent clumping (Fig. 11).

Fig. 11. Histology of rat mesenteric vascular bed.
Histology of the rat mesentery preparations from Fig. 10. Several samples of the jejunum were taken. The sections were stained with hematoxylin and eosin and the vessels were assessed by light microscopy
(A-B) ***Rat mesentery perfused with control RBCs (c-RBCs, treated with vehicle)***. **(A)** shows an artery (magnified on **a**) and a vein (magnified on **b**) containing RBCs. **(B)** shows a capillary (magnified on **c**). **(C-H)** ***Rat mesentery perfused with HlyA-exposed RBCs (HlyA-RBCs)***. Pictures show an artery **(C)**, veins **(D-E)** and cappilaries **(F-H)** containing RBCs.and
The paraffin embedded preparations are representative from several experiments.

3.13 Deformability

Deformability changes of c-, Pro-, HlyAΔ914-936- and HlyA-RBCs were analyzed by ektacytometry, which quantifies the magnitude of cell elongation as a function of applied osmolality (80-690 mosm/kg), or as a function of shear stress (0.2-30 Pa).

When the elongation index (EI) was measured at gradually changing osmolality but constant shear stress, it produced characteristic osmoscan curves shown in Fig. 12 A.

Fig. 12. Effect of HlyA and protein analogs on RBCs deformability.
(A) Deformability vs osmolality. Deformability (elongation index, EI) of RBCs as a function of applied osmolality (80-690 mOsm/Kg) at constant shear stress (30 Pa). Before measurements, RBCs suspensions (40% hematocrit) were exposed to HlyA, ProHlyA, HlyAΔ914-936 or vehicle (Control), for 2.5 min or 3.5 min. ***(B) Deformability vs shear stress***. EI values of RBCs as function of shear stress (0.2-30 Pa), at constant iso-osmolarity. Prior to measurements, RBCs suspensions (44% hematocrit) were exposed for 5 min to ProHlyA (*N*=4), HlyA (*N*=8), HlyAΔ914-936 (*N*=1) or vehicle (Control, *N*=9). Upper and lower panels show reconstructed-images of the shape of Control and HlyA-treated RBCs, respectively, at different values of shear stress. Results are mean values ± S.E.M. Numbers of independent preparations (*N*) are indicated. HlyA, ProHlyA and HlyAΔ914-936 concentrations were adjusted as indicated before.

The maximum point of the curves (EI max) represents the osmolality at which cells have the highest deformability. EI can decrease on both arms of the curve by either a reduction in surface area-to-volume ratio (S/V) or an increase in intracellular viscosity (59).

As expected, for c-RBCs the curve exhibited a maximum near 320 mOsM, suggesting that they deformed optimally in isosmolar conditions. Pro-RBCs and HlyAΔ914-936-RBCs showed a similar response. In HlyA-RBCs the toxin time-dependently shifted the curve to the right. This is indicative of HlyA-RBCs increasing Vt and sphericity and reducing the cellular viscosity determined by the intracellular hemoglobin concentration. Thus a higher osmolality (O hyper) was required to achieve a similar deformability to that observed with c- and Pro-RBCs (Suppl. Fig. 7).

In a second series of experiments, EI was tested as a function of shear stress in isosmotic conditions. C-RBCs, Pro-RBCs and HlyAΔ914-936-RBCs showed a non-linear increase of EI as a function of shear stress. This is compatible with RBCs extending their long axis with the flow, as the shape changes from an oblate-like spheroid to a prolate-like ellipsoid (Fig. 12 B). HlyA-RBCs, on the other hand, had a relatively low EI at all levels of applied shear stresses, probably reflecting that cells were not prone to form ellipsoids, as simulated images illustrate (insets of Fig. 12 B).

3.14 Aggregability

In typical syllectograms, a refraction index (Isc) depends on the interaction forces between two adjacent RBCs, which in turn vary with viscosity, cell shape and membrane damage. Experiments were run in the presence of dextran (400 kDa), which mimics viscous effect of plasma proteins. Aggregates are dispersed with increasing shear forces, and reform under low shear force conditions. In c- and Pro-RBCs, roughly similar syllectograms were obtained; an increase in Isc (upstroke) was observed when, after the rotor stopped, RBCs were assumed to retake their normal shape and orient randomly. This was followed by a decrease in Isc values when cells aggregated (Fig. 13 A). Pro-RBCs usually adopt an echinocyte-like shape (Fig. 7 D), which may induce higher interaction forces between pairs of cells, thereby explaining the higher Isc values a t =0.

Fig. 13. Effect of HlyA on aggregability of RBCs
(A) Syllectograms. Refraction index (Isc) *vs* time. Before measurements, RBCs suspensions (40 % hematocrit) were exposed to HlyA, ProHlya or vehicle (Control) for 5 min, an aggregability was measured in the presence of 3 % dextran 400 (400 kDa) by light scatter. Results are mean values ± S.E.M. (*N*=7). **(B-D)** ***Micrographies by optical microscopy*** of RBCs treated with vehicle (**B**), ProHlyA (**C**) and HlyA (**D**), in the presence of 3 % dextran 40X.
Numbers of independent preparations (*N*) are indicated.

In contrast, the HlyA-RBCs curve was flat. In line with osmoscans showing higher O hyper values (Suppl. Fig. 7) and the observed swelling (Fig. 3), HlyA-RBCs are assumed to be more spherical, thus decreasing contact area between adjacent cells and refracting the laser in a lesser extent, thereby yielding the observed small Isc values. HlyA-RBCs were not able to recover their normal shape, nor could they aggregate.
To account for morphological changes, similarly treated RBCs suspensions containing dextran 400 were observed by light microscopy at 40X magnification (Fig. 13 B-D), showing typically stacked RBC from c-RBC (Fig. 13 B); echinocyte-lyke shape from Pro-RBCs (Fig. 13 C), and spherocyte-like shape from HlyA-RBCs (Fig. 13 D).

4. Discussion

HlyA of uropathogenic strains of *E. coli* is known to interact with RBCs in the intravascular milieu, triggering ATP release and metabolic changes leading to hemolysis (19,60). In this context, the main goal of this study was to identify the key factors controlling ATPe kinetics of RBCs exposed to HlyA, and to explore how these changes influence the behavior of RBCs exposed to different environments mimicking several features found *in vivo*. Accordingly, we first assessed ATPe hydrolysis and intracellular ATP release, and its modulation by purinergic receptors and Vt, and then analyzed how HlyA affects metabolic and rheological properties of RBCs suspensions, the adhesion of RBCs to endothelial platforms, and ATP release of RBCs perfused through a heterologous mesentery.

4.1 ATPe regulation

Exposure of RBCs to low concentrations of HlyA led to acute ATP release and hemolysis. In addition, ATPe was hydrolyzed by intracellular ATPases of lyzed RBCs and ectoATPase activity of RBCs. By fitting a data driven model to experimental data of ATPe kinetics, lytic ATP release, ectoATPase activity and intracellular ATPase activity, we were able to calculate the non-lytic component of ATP release, and quantify the relative contribution of each of these processes to ATPe kinetics.

This analysis showed that ATPe kinetics of HlyA-RBCs was mainly governed by simultaneous lytic and non-lytic ATP release. Enzymatic ATPe hydrolysis was relative low at acute exposures times. This is consistent with low hemolysis and therefore low ATPe hydrolysis by intracellular ATPases, together with relatively low ectoATPase activity, which is a feature of mature RBCs from mammalian species, including humans (32,42,61). There may be more than one ENTPDase accounting for ectoATPase activity (62,63), whereas no ectophosphatase activity was detected in RBCs (64).

Despite low ATPe hydrolysis, since under HlyA exposure [ATPe] increases continuously and ectoATPase and intracellular ATPase activities are linearly dependent on [ATPe], their contribution to ATPe kinetics is higher at high incubation times, causing reductions of up to 22 % at the end of the experiments.

The contribution to ATPe hydrolysis by ectoATPase activity could be even higher since, as we showed before (42) ATP at the cell surface, where the active sites of ectonucleotidases are located, is 2.4 higher than bulk ATPe measured in RBCs assay medium.

In addition to direct [ATPe] decrease by enzymatic hydrolysis, we and others have shown that the resulting ADPe can activate P2Y13 receptors mediating a decrease of cAMP content, coupled to reduced ATP release (29,33). Although, as show in this study, ATPe to ADPe conversion might be very low in RBCs, while ectoADPase activity is relatively high (64), *in vivo* intravascular ATP hydrolysis by plasma exoenzymes, ectonucleotidases of other blood cell types or the vascular wall might provide sufficient ADPe to promote inactivation of ATP release of RBCs (65).

4.2 Non-lytic ATP release

To characterize non-lytic ATP efflux (J_{NL}), we first compared the effects of HlyA and ProHlyA, the un-acylated precursor of HlyA. In rabbit RBCs ProHlyA is able to insert into cell membranes (50). However, acylation at internal lysines K563 and K689 –turning ProHlyA into HlyA- was

necessary for the toxin to become hemolytic (66). The observed absence of ATP release with ProHlyA in this study suggests that acylation is also important to trigger non-lytic ATP exit from RBCs. Although the role of toxin acylation remains unclear, studies on the effects of chemical denaturants, ANS binding and sensitivity to proteases suggest that HlyA –unlike ProHlyA- may expose intrinsically disordered regions mediating intracellular signaling leading to hemolysis (50,66). This is in line with our results showing that HlyA, but not ProHlyA, was able to irreversibly externalize PS and increase cytosolic Ca^{2+} of RBCs, two events coupled to eryptosis (67). Alternatively, FRET experiments using label toxins showed that HlyA, but not ProHlyA, was able to oligomerize on ghost erythrocytes membranes suggesting that these disordered regions might promote protein-protein interactions, controling the oligomerization of the toxin (68). An oligomer, in turn, should create a 2-3 nm pore capable of mediating ATP efflux from RBCs (69). However, the existence of such a pore has been challenged due to lack of direct evidence by electron microscopy or crystal structure analysis (24,25).

Thus, to test if HlyA induced ATP release by direct interaction with the phospholipid membrane, with no other proteins involved, we exposed HlyA to liposomes loaded with ATP. We used liposomes composed of PC:SM:Cho mimicking the composition of the outer hemilayer of RBCs (51). This lipid mixture presents liquid order domains similar to the membrane microdomains involved in oligomerization and the lytic mechanism of the toxin (68,70). Although HlyA was reported to promote efflux of fluorochromes and even ATP from liposomes (10,71), the magnitude of this flux was not assessed. In our hands, using PC:SM:Cho liposomes, ATP efflux mediated by high HlyA concentrations was measurable, but very low, when compared to similar results using HlyA-RBCs. Thus, even if HlyA can indeed form an oligomeric pore liposomes, our results imply that the toxin is not forming an ATP conduit.

Thus, it seems that HlyA effect on ATP release may require the interaction with endogenous membrane proteins of RBCs. HlyA was found to bind to N-linked oligosaccharides to their β2-integrin receptors (72), raising the possibility that binding of the toxin to various cells might occur through the recognition of glycosylated membrane components, such as gangliosides and glycoproteins. We then exposed RBCs to HlyAΔ914-936, a deletion analog protein unable to bind glycophorins, a highly abundant family of membrane proteins of RBCs. A previous study showed that HlyAΔ914-936 was not hemolytic on RBCs, and that the peptide Trp914–Arg936 had no lytic activity on RBCs, although it could bind to glycophorins in reconstituted liposomes (26).

Again, as with ProHlyA, although HlyAΔ914-936 induced RBCs crenation in the absence of Ca^{2+}i increase, it neither alters [ATPe] nor hemolysis. In HlyA-RBCs, on the contrary, a steep acute Ca^{2+}i increase correlated with a crenatocyte to spherocyte transition, followed by hemolysis. This means that, at least for RBCs, glycophorins seem important for HlyA activity, although other proteins might as well be interacting with the toxin. These results are also in agreement with the need of higher concentration of HlyA to induce detectable ATP release from liposomes.

In looking for endogenous ATP transport systems, we analyzed the role of pnx1, an ubiquitous ATP conduit in cells (18). Particularly, we tested the effect of CBX, a glycyrrhetinic acid derivative known to inhibit pnx1 in a wide variety of cell types (73,74). Pnx1 was predicted to form four α-helical transmembrane domains exposing two extracellular loops, with multiple residues in the first extracellular loop mediating CBX dependent pnx1 inhibition (75). In RBCs, CBX sensitive pnx1 acts as a conduit for ATP efflux of RBCs challenged by amphipatic peptides,

swelling, hypoxia and beta adrenergic stimulation (32,42,75,76). However, in HlyA-RBCs the effects of CBX can be more complex since, as we observed in this study, CBX exposure led to a parallel inhibition of [ATPe] and hemolysis of HlyA-RBCs. This is compatible with the model of Fig. 14, since a decrease of J_{NL} (by CBX blockage in this case) can diminish swelling and therefore decrease the extent of hemolysis.

We then simulated the effect of CBX on ATP efflux of viable cells (i.e, J_{NL}). Predictions showed that J_{NL} is composed of two fluxes, a CBX-sensitive (presumably pnx1) and CBX-tolerant flux. CBX reduction of J_{NL} was low in the early phase of toxin exposure (≈20 % at 5min), but high at late exposure times (≈80 % at 10 min) (Suppl. Fig. 3).

4.3 Interaction between cell volume and [ATPe]

Analyzing changes in Vt induced by HlyA is important for various reasons. First, HlyA activity in RBCs has been associated with changes in Vt (60). Second, hypo- and isosmotic swelling are strong inducers of non-lytic ATP release from RBCs (32,73,77), while excessive swelling can induce hemolysis, thereby activating lytic ATP efflux. Third, we observed before that treating RBCs with an amphipatic peptide induced interacting changes of [ATPe] and Vt (33).

Results of this study showed that following HlyA exposure, RBCs slightly crenate and shrunk during the first min, followed by continuous swelling, which preceded a steep increase in hemolysis.

As volume histograms (Suppl. Fig. 4), volume kinetics (Fig. 3 A) and morphology dynamics (Fig. 7 B-C) show, the accompanying Vt and shape changes of RBCs are heterogeneous, both within a single RBCs sample, and between samples from different individuals. This is because RBCs, with its limited lifespan, represent an heterogeneous population expressing different molecules as they age. In addition, polymorphisms of P2X2-P2X7 receptors from RBCs (78) may contribute to variations in Vt kinetics of RBCs samples from different individuals, particularly in the context of the observed P2X dependent swelling.

The biphasic Vt kinetics was also reported by Skals et al. (60), who showed that $Ca^{2+}i$ increase led to net KCl efflux mediated by KCa3.1 and TMEM16A channels, causing the shrinking phase, while subsequent swelling was assumed to be caused by sodium uptake. An early phase dominated by K^+ conductance, followed by a late phase dominated by Na^+ conductance, is compatible with our results showing a hyperpolarization followed by a depolarization of the membrane potential, with roughly similar kinetics to that of Vt.

Since swelling *per se* is known to activate ATP exit of RBCs (32,73), we tested the extent to which HlyA induced ATP release depends on the observed swelling, and the underlying causative relationships linking changes in Vt and [ATPe].

Next, we analyzed the extent to which swelling promotes ATP release. When HlyA was added in a hyperosmotic medium to counteract swelling, ATPe release was highly inhibited. Interestingly, according to osmoscans, hyperosmotic conditions allowed HlyA-RBCs to regain elongation of untreated cells. Thus, swelling mediated most of HlyA triggered ATP release. We then tested whether ATPe could affect swelling. We first found that pre-incubation with excess apyrase, an ATPe remover (30,53), did not alter swelling. However, experiments testing apyrase activity in the absence of cells showed that, even if this enzyme reduced [ATPe] dose-dependently, ATPe was still present in the medium for several minutes. This transient presence of ATPe could be sufficient to trigger purinergic signaling. In particular, ATPe is the only natural ligand of ionotropic P2X receptors, of which RBCs exhibit functional P2X2 and P2X7 subtypes

(54,55) . P2X7 receptors are more abundant than P2X2 on RBCs (54), but exhibit much lower affinity for ATP (79).

Activation of these receptors may lead to the net transport of cations altering intracellular osmolarity and therefore Vt (80). Pre-incubation with antagonists of either P2X7 or P2X1-2, reduced HlyA dependent [ATPe] increase by 52-73 %, and hemolysis by 53-66 %. Thus, as with CBX, these blockers inhibited both the lytic and the non-lytic component of ATP release. Moreover, P2X blockage strongly reduced swelling. Thus P2X receptors are working as a bridge, connecting swelling with activation of ATP release. The fact that P2X antagonists were unable to block $Ca^{2+}i$ uptake precludes their participation in the early shrinking phase of the volumetric response.

4.4 Adhesion

Although RBCs do not adhere to vascular endothelial cells under physiological conditions, adherence occurs in many pathologies associated with vascular occlusion (67,81). During UPEC infection, when HlyA is produced and released in the intravascular space, the onset of inflammatory processes may up-regulate various adhesive molecules of endothelial cells (60), while eryptosis induced by HlyA, with concomitant PS externalization (as observed in this study), might turn RBCs more adhesive. This possibility is particularly important in the context of ATPe regulation of RBCs (analyzed in (82)), since we observed before that adhesion of these cells to chemically different adherent molecules positively modulates the activation of ATP release by swelling (32). To mimic this scenario, we perfused HlyA-RBCs at various controlled flows through artificial vessels coated with activated HMEC cells. Adhesion of HlyA-RBCs was very high at low flow. However, adhesive forces were weak, as increments in flow led to almost full detachment from HMEC cells. This means that, under HlyA exposure, PS externalization of RBCs might correlate with their higher adhesion to vascular endothelial cells, particularly in regions of low flow. However weak adhesion should not lead to vascular occlusion.

4.5 Rat mesenteric vascular bed. Monitoring lytic and non-lytic ATP release

Since HlyA can induce ATP exit by lytic and non-lytic mechanisms, can this response be observed in a vascular system? To answer this question, we used a rat mesentery model where the entire mesenteric vascular system and the irrigated small intestine remained intact, and HlyA-RBCs (*vs.* c- and Pro-RBCs) were perfused at controlled flow. In this heterologous system intravascular pressure can change, and mechanical forces due to peristaltic movements can occur.

When HlyA-RBCs were perfused, significant increases of intravascular ATP (ATPiv) and Hb were observed, while Pro-RBCs induced much lower responses. As observed before when assessing [ATPe] of isolated RBCs suspensions, [ATPiv] increments were due to lytic and non-lytic components of ATP release. Since no damage to the endothelium occurred and HlyA alone did not change [ATPiv], the observed elevated [ATPiv] should derive mostly from intracellular ATP of RBCs.

Higher [ATPiv] increases than observed could be expected *in vivo*, where hematocrits are about 3-fold higher than that used in our experimental setup. Moreover, the accumulated ATPiv can underestimate ATP release by HlyA-RBcs, since in the vascular environment the nucleotide can have various fates. I.e., it can act as a substrate for ecto- and exonucleotidases

and phosphatases of plasma, blood cells and the vascular endotelium (55,62,65), generating various di- and trinucleotides, and adenosine. These compounds may bind purinergic receptors mediating a variety of responses (55,83). In particular, ATPe to ADPe conversion, promoting elevated intravascular ADP, might activate thrombocytes, so that HlyA might potentiate thrombocyte aggregation and pro-coagulation, thereby leading to thrombosis episodes (10). In addition, as our group and others have shown before, *E. coli* can take up and metabolize exogenous ATP (84,85), a process incrementing the energetic status of bacteria. Thus, since intravascular UPEC produce HlyA, some of these processes might be relevant during progression of the infection.

4.6 Deformability and aggregability of HlyA-RBCs

RBCs acutely crenated when challenged by ProHlyA or HlyA. In addition HlyA, unlike ProHlyA, induced increments of cytosolic Ca^{2+} and PS externalization. Moreover, the mutually activating loop coupling increments of [ATPe] and Vt triggered irreversible swelling. All these changes may have altered the rheological properties of HlyA-RBCs, with consequences on blood flow.

We thus monitored changes in deformability when HlyA-RBCs were exposed to shear stress or osmolality gradients. These stimuli are relevant *in vivo*, since RBCs are mobile cells exposed to mechanical forces when passing through small capillaries of the circulation and/or to osmotic gradients, especially in the kidney (86). Additionally we monitored HlyA-RBCs aggregability, since plasma proteins may render RBCs more liable to aggregate, particularly under low flow, causing vascular obstruction.

Osmoscan curves were roughly similar for c- HlyAΔ914-936- and Pro-RBCs. However, in HlyA-RBCs, a significant right-shift of the osmoscan was observed, suggesting increased sphericity and swelling, and consequently reduced cellular viscosity.

We then tested deformability as a function of shear stress. C-, HlyAΔ914-936- and Pro-RBCs exhibited large scale deformations, implying that the long axis of the cell extended with increased shear rates. In contrast, HlyA-RBCs displayed low deformability under similar conditions, which agrees well with the increment of ceramide contents in the outer leaflet of RBC membrane treated with the toxin, as previously demonstrated (20). Thus, HlyA-RBCs should be less capable to deform in narrow vessels, and as swollen cells more fragile to hypotonic stress. On the other hand, less deformable cells exposing PS may foster engulfment by phagocytes and potential clearance from the circulation (87).

We then turned our attention to HlyA-RBCs aggregation. The tendency of RBCs to aggregate is an important determinant of blood viscosity. Aggregates are dispersed with increasing shear forces, and reform under low-flow conditions. Thus, *in vivo* aggregation affects the fluidity of blood, especially in the low-shear regions of the circulatory system (88,89).

In syllectograms, c- and Pro-RBCs behaved roughly similar. I.e., basal Isc values were compatible with complete disaggregation at moderate shear rate and upstroke signal was compatible with RBCs recovering their normal shape and orientating randomly. This was followed by a time dependent decrease of Isc, reflecting aggregation. In this and other studies (50) Pro-RBCs were shown to adopt an echinocyte shape, which may induce higher interaction forces between pair of cells and thus explain the higher Isc values at t=0.

In contrast, HlyA-RBCs syllectograms were flat, suggesting no changes in shape during upstroke. In line with osmoscans showing low elongation and Vt kinetics and volumetric

histograms showing swelling, HlyA-RBCs are assumed to be more spherical, thus decreasing contact area between adjacent cells, which may explain the observed reduced aggregation.

4.7 Summarizing main findings

Main results are depicted in Fig. 14. HlyA is activated by acylation of ProHlyA (1). The acylated moiety, as well as the glycophorin binding site of HlyA (absent in HlyAΔ914-936) proved to be important for toxin activity (2). HlyA triggered simultaneous lytic and non-lytic ATP release (3), both using isolated RBCs, or RBCs suspensions flowing through a rat mesentery model, leading to increased [ATPe]. This increase was in part counteracted by ATPe hydrolysis due to ectoATPase activity (4), and to ATPase activity of lysed cells (5). Binding of ATPe to P2X (6) triggered progressive swelling (7), which correlates with higher cell sphericity and lower deformability under osmotic gradients and shear stress, and low aggregability in viscous media. Low swelling activated mainly non-lytic ATP release, while high swelling produced hemolysis, leading to lytic ATP release and increases of MABP under flow. Swelling and hemolysis transduce into further increases of [ATPe], closing the signaling circuit.

Fig 14: Regulation of ATPe in HlyA-exposed RBCs, and its modulation by cell volume and hemolysis
Exposure to HlyA induces ATP release by lytic (J_L) and non-lytic (J_{NL}) mechanisms, causing [ATPe] increase, which is partially counteracted by ATPe hydrolysis due to ectoATPase (J_{EA}) and intracellular ATPase (J_{IA}) activities. ATPe activates P2X receptors coupled to cell swelling (Vt). Swelling below a critical volume Vc (Vt<Vc) activates J_{NL}, favoring a higher symmetry (Fig 12) and lower aggregability (Fig. 13) of RBCs. Values of Vt>Vc lead to hemolysis and activation of J_L; likewise, hemolysis can release intracellular ATPases, thereby activating J_{IA}, which decreases [ATPe]. Finally, in a mesenteric system, hemolysis can increase intravascular pressure (MABP).
The effects described above are absent when RBCs are treated with ProHlyA and HlyAΔ914-936.
ATPi and ATPe denote intracellular and extracellular ATP, respectively.

Hemolysis provided two processes ameliorating the effects of the loop; dying cells will decrease the amount of cells activating non-lytic ATP release and simultaneously release intracellular ATPases capable of decreasing [ATPe]. According to the scheme cell death, by promoting [ATPe] increase, can signal P2X receptors of surviving cells, modulating the reciprocal regulation of ATPe and Vt.
To the extent that P2X blockers break the signaling loop promoting RBCs hemolysis, they –or improved variants- may offer a protection mechanism against HlyA hemolysis in UPEC infected patients.

Acknowledgements

M.F.L.D., C.L.A., R.G.L., M.V.E., V.M, V.H., and P.J.S. are career researchers at Consejo Nacional de Investigaciones Científicas y Técnicas (CONICET). N.L. is a doctoral student from Universidad de Buenos Aires. M.A.O. and S.D.L. are full professor and assitant professor, respectively, at Paris Diderot University. C.M.G. is a researcher at Universidad Nacional Autónoma de México.

We thank Dr. H. Ostolaza for kindly providing us with the plasmid for HlyAΔ914-936 and Dr. Welch for kindly providing *E. coli* strains WAM 1824 and WAM 783. We are thankful to R. C. Mario for assistance with the histological techniques, Dr. J. Lofeudo for providing Sprague-Dawley rats; M. Marin for helping with experiments using the adhesion platform, C. Hattab for experimental assistance, Dr. S. Verstraeten for advice with the techniques to measure membrane potential, Dr. V Rivarola and C. Capurro for providing us with the cell scepter to evaluate cell volume distributions, Dr. L. Galizia for helpful discussions on main results, M. Sacerdoti and S. Venerus for preliminary results on ATP release and luciferase calibrations and Dr. M. Manzi for assistance in designing the scheme of Fig. 14. We thank Dra. M. Pucci Molineris for assistance in image processing.

Funding

This work was supported by the Consejo Nacional de Investigaciones Científicas y Técnicas (Grant PIP 112 20110100639 and Grant PDTS/CIN 2014 193); the Universidad de Buenos Aires (Grant 200201701001 52BA); the Agencia Nacional de Promoción Científica y Técnica (Grant PICT 2014-0327, Grant PICT 2016-1041 and Grant ECOS Sud A15S01); the Laboratory of Excellence GR-Ex (Grant ANR-11-LABX-0051). The funders had no role in study design, data collection and analysis, decision to publish, or preparation of the manuscript.

Author contribution

P.J.S formulated the project.

M.F.L.D., S.D.L., N.L., C.L.A., V.M., M.A.O., V.H., and P.J.S. conceived and designed the experiments.

M.F.L.D., S.D.L, V.H., M.A.O. and P.J.S. gave advice on experimental design and hypothesis.

M.F.L.D., N.L, C.L.A., S.D.L., M.V.E., N.E., D.E.R., L.E.V., V.M., M.A.O., V.H. and P.S. performed the experiments.

M.F.L.D., N.L., C.L.A., S.D.L., V.M., M.A.O., V.H., N.E., D.E.R. and P.J.S. analyzed the data.

R.G.L. designed the mathematical algorithm

M.F.L.D., M.A.O., V.M., V.H. and P.J.S. contributed reagents-materials.-analysis tools.

M.F.L.D. and P.J.S. wrote the manuscript.

All authors reviewed and approved the manuscript.

References

1. Ellsworth ML, Ellis CG, Sprague RS. Role of erythrocyte-released ATP in the regulation of microvascular oxygen supply in skeletal muscle. Acta Physiol. 2016;216(3):265–76.
2. Wan J, Ristenpart WD, Stone HA. Dynamics of shear-induced ATP release from red blood cells. Proc Natl Acad Sci [Internet]. 2008;105(43):16432–7. Available from: http://www.pnas.org/cgi/doi/10.1073/pnas.0805779105
3. González-Alonso J, Olsen DB, Saltin B. Erythrocyte and the regulation of human skeletal muscle blood flow and oxygen delivery: role of circulating ATP. Circ Res [Internet]. 2002 Nov 29 [cited 2015 Aug 7];91(11):1046–55. Available from: http://www.ncbi.nlm.nih.gov/pubmed/12456491
4. Sprague RS, Bowles EA, Achilleus D, Ellsworth ML. Erythrocytes as controllers of perfusion distribution in the microvasculature of skeletal muscle. Acta Physiol (Oxf) [Internet]. 2011 Jul [cited 2015 Aug 7];202(3):285–92. Available from: http://www.pubmedcentral.nih.gov/articlerender.fcgi?artid=3021763&tool=pmcentrez&rendertype=abstract
5. Ellsworth ML, Sprague RS. Regulation of blood flow distribution in skeletal muscle: role of erythrocyte-released ATP. J Physiol [Internet]. 2012 Oct 15 [cited 2015 Aug 7];590(Pt 20):4985–91. Available from: http://www.pubmedcentral.nih.gov/articlerender.fcgi?artid=3497557&tool=pmcentrez&rendertype=abstract
6. Hellsten Y, Nyberg M, Mortensen SP. Contribution of intravascular versus interstitial purines and nitric oxide in the regulation of exercise hyperaemia in humans. J Physiol [Internet]. 2012 Oct 15 [cited 2015 Aug 7];590(Pt 20):5015–23. Available from: http://www.pubmedcentral.nih.gov/articlerender.fcgi?artid=3497560&tool=pmcentrez&rendertype=abstract
7. Sprague RS, Ellsworth ML, Stephenson a H, Kleinhenz ME, Lonigro a J. Deformation-induced ATP release from red blood cells requires CFTR activity. Am J Physiol. 1998;275(5 Pt 2):H1726–32.
8. Sprague RS, Stephenson AH, Bowles E a., Stumpf MS, Lonigro AJ. Reduced expression of Gi in erythrocytes of humans with type 2 diabetes is associated with impairment of both cAMP generation and ATP release. Diabetes [Internet]. 2006 Dec [cited 2015 Aug 3];55(12):3588–93. Available from: http://www.ncbi.nlm.nih.gov/pubmed/17130508
9. Sprague RS, Bowles EA, Achilleus D, Stephenson AH, Ellis CG, Ellsworth ML. A selective phosphodiesterase 3 inhibitor rescues low PO2-induced ATP release from erythrocytes of humans with type 2 diabetes: implication for vascular control. Am J Physiol Heart Circ Physiol [Internet]. 2011 Dec 1 [cited 2015 Aug 5];301(6):H2466-72. Available from: http://ajpheart.physiology.org/content/301/6/H2466.short
10. Skals M, Bjaelde RG, Reinholdt J, Poulsen K, Vad BS, Otzen DE, et al. Bacterial RTX toxins allow acute ATP release from human erythrocytes directly through the toxin pore. J Biol Chem [Internet]. 2014 Jul 4 [cited 2015 Dec 16];289(27):19098–109. Available from: http://www.pubmedcentral.nih.gov/articlerender.fcgi?artid=4081947&tool=pmcentrez&rendertype=abstract
11. Alvarez CL, Schachter J, De Sá Pinheiro AA, De Souza Silva L, Verstraeten S, Persechini PM, et al. Regulation of extracellular ATP in human erythrocytes infected with Plasmodium falciparum. PLoS One [Internet]. Public Library of Science; 2014 Jan 23 [cited 2015 Jul 31];9(5):e96216. Available from: http://dx.plos.org/10.1371/journal.pone.0096216
12. Sikora J, Orlov SN, Furuya K, Grygorczyk R. Hemolysis is a primary ATP-release mechanism in human erythrocytes. Blood. 2014;124(13):2150–7.
13. Lazarowski ER. Vesicular and conductive mechanisms of nucleotide release. Purinergic

Signal. 2012;8(3):359–73.
14. Islam MR, Uramoto H, Okada T, Sabirov RZ, Okada Y. Maxi-anion channel and pannexin 1 hemichannel constitute separate pathways for swelling-induced ATP release in murine L929 fibrosarcoma cells. Am J Physiol Cell Physiol [Internet]. 2012 Nov 1 [cited 2015 Aug 7];303(9):C924-35. Available from: http://www.ncbi.nlm.nih.gov/pubmed/22785119
15. Marginedas-Freixa I, Alvarez CL, Moras M, Leal Denis MF, Hattab C, Halle F, et al. Human erythrocytes release ATP by a novel pathway involving VDAC oligomerization independent of pannexin-1. Sci Rep [Internet]. 2018;8(1):1–13. Available from: https://www.nature.com/articles/s41598-018-29885-7
16. Marginedas-Freixa I, Alvarez C, Moras M, Hattab C, Bouyer G, Chene A, et al. Induction of ATP Release, PPIX Transport, and Cholesterol Uptake by Human Red Blood Cells Using a New Family of TSPO Ligands. Int J Mol Sci [Internet]. Multidisciplinary Digital Publishing Institute; 2018 Oct 10 [cited 2018 Oct 30];19(10):3098. Available from: http://www.mdpi.com/1422-0067/19/10/3098
17. Di Virgilio F, Schmalzing G, Markwardt F. The Elusive P2X7 Macropore. Trends Cell Biol [Internet]. Elsevier Ltd; 2018;28(5):392–404. Available from: http://dx.doi.org/10.1016/j.tcb.2018.01.005
18. Wang J, Dahl G. Pannexin1: a multi-function and multi-conductance/-permeability membrane channel. Am J Physiol Physiol [Internet]. American Physiological Society Bethesda, MD ; 2018 May 2 [cited 2018 Jun 14];ajpcell.00302.2017. Available from: http://www.physiology.org/doi/10.1152/ajpcell.00302.2017
19. Skals M, Jorgensen NR, Leipziger J, Praetorius HA. -Hemolysin from Escherichia coli uses endogenous amplification through P2X receptor activation to induce hemolysis. Proc Natl Acad Sci [Internet]. 2009 Mar 10 [cited 2015 Dec 16];106(10):4030–5. Available from: http://www.pubmedcentral.nih.gov/articlerender.fcgi?artid=2656199&tool=pmcentrez&rendertype=abstract
20. Velásquez Carrizo F, Maté S, Bakás L, Herlax V. Induction of eryptosis by low concentrations of E. coli alpha-hemolysin. Biochim Biophys Acta - Biomembr [Internet]. Elsevier B.V.; 2015 [cited 2016 Jul 9];1848(11):2779–88. Available from: http://dx.doi.org/10.1016/j.bbamem.2015.08.012
21. Hughes C, Hacker J, Roberts A, Goebel W. Hemolysin Production As a Virulence Marker in Symptomatic and Asymptomatic Urinary-Tract Infections Caused By Escherichia-Coli. Infect Immun. 1983;39(2):546–51.
22. Marrs CF, Zhang L, Foxman B. Escherichia coli mediated urinary tract infections: Are there distinct uropathogenic E. coli (UPEC) pathotypes? FEMS Microbiol Lett. 2005;252(2):183–90.
23. Herlax V, Bakás L. Acyl chains are responsible for the irreversibility in the Escherichia coli α-hemolysin binding to membranes. Chem Phys Lipids [Internet]. 2003 [cited 2017 Jun 26];122(1–2):185–90. Available from: http://www.sciencedirect.com/science/article/pii/S0009308402001913
24. Benz R, Maier E, Bauer S, Ludwig A. The deletion of several amino acid stretches of Escherichia coli alpha-hemolysin (HlyA) suggests that the channel-forming domain contains beta-strands. PLoS One. 2014;9(12):1–26.
25. Wang Y, Wang S. Increased extracellular ATP: an omen of bacterial RTX toxin-induced hemolysis? Toxins (Basel). 2014;6(8):2432–4.
26. Cortajarena AL, Goñi FM, Ostolaza H. A receptor-binding region in Escherichia coli α-haemolysin. J Biol Chem. 2003;278(21):19159–63.
27. Carroll J, Raththagala M, Subasinghe W, Baguzis S, D'Amico Oblak T, Root P, et al. An altered oxidant defense system in red blood cells affects their ability to release nitric oxide-stimulating ATP. Mol Biosyst. 2006;2(6):305–11.

28. Koziak K, Sévigny J, Robson S, Siegel J, Kaczmarek E. Analysis of CD39/ATP Diphosphohydrolase (ATPDase) Expression in Endothelial Cells, Platelets and Leukocytes. Thromb Haemost [Internet]. Schattauer GmbH; 1999 Dec 9 [cited 2018 Jun 14];82(11):1538–44. Available from: http://www.thieme-connect.de/DOI/DOI?10.1055/s-0037-1614868
29. Wang L, Olivecrona G, Götberg M, Olsson ML, Winzell MS, Erlinge D. ADP acting on P2Y13 receptors is a negative feedback pathway for ATP release from human red blood cells. Circ Res. 2005;96(2):189–96.
30. Pafundo DE, Alvarez CL, Krumschnabel G, Schwarzbaum PJ. A volume regulatory response can be triggered by nucleosides in human erythrocytes, a perfect osmometer no longer. J Biol Chem [Internet]. 2010 Feb 26 [cited 2015 Aug 7];285(9):6134–44. Available from: http://www.pubmedcentral.nih.gov/articlerender.fcgi?artid=2825408&tool=pmcentrez&rendertype=abstract
31. Erlinge D, Burnstock G. P2 receptors in cardiovascular regulation and disease. Purinergic Signal [Internet]. 2008 Mar [cited 2015 Jun 29];4(1):1–20. Available from: http://www.pubmedcentral.nih.gov/articlerender.fcgi?artid=2245998&tool=pmcentrez&rendertype=abstract
32. Leal Denis MF, Incicco JJ, Espelt MV, Verstraeten S V., Pignataro OP, Lazarowski ER, et al. Kinetics of extracellular ATP in mastoparan 7-activated human erythrocytes. Biochim Biophys Acta - Gen Subj [Internet]. Elsevier B.V.; 2013 [cited 2018 Jun 15];1830(10):4692–707. Available from: http://dx.doi.org/10.1016/j.bbagen.2013.05.033
33. Leal Denis MF, Alvarez HA, Lauri N, Alvarez CL, Chara O, Schwarzbaum PJ. Dynamic regulation of cell volume and extracellular ATP of human erythrocytes. PLoS One. 2016;11(6).
34. Moayeri M, Welch RA. Prelytic and Lytic Conformations of Erythrocyte-Associated Escherichia coli Hemolysin. Infect Immun [Internet]. 1997 [cited 2018 Jun 4];65(6):2233–9. Available from: https://www.ncbi.nlm.nih.gov/pmc/articles/PMC175308/pdf/652233.pdf
35. Boehm DF, Welch RA, Snyder ' IS. Domains of Escherichia coli Hemolysin (HlyA) Involved in Binding of Calcium and Erythrocyte Membranes. Infect Immun [Internet]. 1990 [cited 2018 Jun 4];1959–64. Available from: http://iai.asm.org/content/58/6/1959.full.pdf
36. Bradford MM. A rapid and sensitive method for the quantitation of microgram quantities of protein utilizing the principle of protein-dye binding. Anal Biochem [Internet]. Academic Press; 1976 May 7 [cited 2018 Jun 15];72(1–2):248–54. Available from: https://www.sciencedirect.com/science/article/pii/0003269776905273?via%3Dihub
37. Strehler BL. Bioluminescence assay: principles and practice. Methods Biochem Anal [Internet]. 1968 Jan [cited 2015 Jun 6];16:99–181. Available from: http://www.ncbi.nlm.nih.gov/pubmed/4385967
38. Brown AM. ATP and ATPase determination in red blood cells. In: Ellory JC, Young J., editors. Red Cell Membranes — A Methodological Approach,. London: Accademic Press; 1982. p. 223–38.
39. Gorman MW, Marble DR, Ogimoto K, Feigl EO. Measurement of adenine nucleotides in plasma. Luminescence [Internet]. Jan [cited 2015 Aug 13];18(3):173–81. Available from: http://www.ncbi.nlm.nih.gov/pubmed/12701093
40. Olearczyk JJ, Stephenson AH, Lonigro AJ, Sprague RS. Heterotrimeric G protein Gi is involved in a signal transduction pathway for ATP release from erythrocytes. Am J Physiol Heart Circ Physiol [Internet]. 2004 Mar 1 [cited 2015 Aug 5];286(3):H940-5. Available from: http://www.ncbi.nlm.nih.gov/pubmed/14615280
41. Sridharan M, Bowles EA, Richards JP, Krantic M, Davis KL, Dietrich KA, et al. Prostacyclin

receptor-mediated ATP release from erythrocytes requires the voltage-dependent anion channel. Am J Physiol Heart Circ Physiol [Internet]. 2012 Mar 1 [cited 2015 Jul 31];302(3):H553-9. Available from: http://www.pubmedcentral.nih.gov/articlerender.fcgi?artid=3353798&tool=pmcentrez&rendertype=abstract

42. Montalbetti N, Leal Denis MF, Pignataros OP, Kobatake E, Lazarowski ER, Schwarzbaum PJ. Homeostasis of extracellular ATP in human erythrocytes. J Biol Chem. 2011;286(44):38397–407.
43. Fischer SL, Fischer SP. Mean Corpuscular Volume. Arch Intern Med [Internet]. American Medical Association; 1983 Feb 1 [cited 2018 Jun 15];143(2):282. Available from: http://archinte.jamanetwork.com/article.aspx?doi=10.1001/archinte.1983.00350020108020
44. Baskurt OK, Boynard M, Cokelet GC, Connes P, Cooke BM, Forconi S, et al. New guidelines for hemorheological laboratory techniques. Clin Hemorheol Microcirc [Internet]. 2009 [cited 2018 Jun 14];42(2):75–97. Available from: http://www.ncbi.nlm.nih.gov/pubmed/19433882
45. Nemeth N, Kiss F, Miszti-Blasius K. Interpretation of osmotic gradient ektacytometry (osmoscan) data: A comparative study for methodological standards. Scand J Clin Lab Invest. 2015;75(3):213–22.
46. Yamada A, Gaja N, Ohya S, Muraki K, Narita H, Ohwada T, et al. Usefulness and Limitation of DiBAC 4 (3), a Voltage-Sensitive Fluorescent Dye, for the Measurement of Membrane Potentials Regulated by Recombinant Large Conductance Ca 2+ -Activated K + Channels in HEK293 Cells. Jpn J Pharmacol [Internet]. 2001 [cited 2018 Jun 14];86:342–50. Available from: https://www.jstage.jst.go.jp/article/jjp/86/3/86_3_342/_pdf/-char/en
47. Céliz G, Alfaro FF, Cappellini C, Daz M, Verstraeten S V. Prunin- and hesperetin glucoside-alkyl (C4–C18) esters interaction with Jurkat cells plasma membrane: Consequences on membrane physical properties and antioxidant capacity. Food Chem Toxicol [Internet]. Pergamon; 2013 May 1 [cited 2018 Jun 14];55:411–23. Available from: https://www.sciencedirect.com/science/article/pii/S0278691513000331?via%3Dihub
48. Stringa P, Romanin D, Lausada N, Papa Gobbi R, Zanuzzi C, Martín P, et al. Gut Permeability and Glucose Absorption Are Affected at Early Stages of Graft Rejection in a Small Bowel Transplant Rat Model. Transplant Direct [Internet]. 2017 Nov [cited 2018 Jun 25];3(11):e220. Available from: http://www.ncbi.nlm.nih.gov/pubmed/29184909
49. Soloaga A, Ostolaza H, Goni FM, De La Cruz F. Purification of E. coli pro-haemolysin and a comparison with the properties of mature a-haemolysin. Eur J Biochem. 1996;422(238):418–22.
50. Vázquez RF, Maté SM, Bakás LS, Muñoz-Garay C, Herlax VS. Relationship between intracellular calcium and morphologic changes in rabbit erythrocytes: Effects of the acylated and unacylated forms of E. coli alpha-hemolysin. Biochim Biophys Acta - Biomembr [Internet]. Elsevier B.V.; 2016;1858(8):1944–53. Available from: http://dx.doi.org/10.1016/j.bbamem.2016.05.013
51. Maté S, Busto J V, García-Arribas AB, Sot JS, Vazquez R, Herlax V, et al. N-Nervonoylsphingomyelin (C24:1) Prevents Lateral Heterogeneity in Cholesterol-Containing Membranes. 2014 [cited 2018 Jun 14]; Available from: https://www.ncbi.nlm.nih.gov/pmc/articles/PMC4070274/pdf/main.pdf
52. Leal Denis MF, Incicco JJ, Espelt MV, Verstraeten S V., Pignataro OP, Lazarowski ER, et al. Corrigendum to “Kinetics of extracellular ATP in mastoparan 7-activated human erythrocytes” [Biochim. Biophys. Acta — Gen. Subj. 1830 (10) (2013) 4692–4707]. Biochim Biophys Acta - Gen Subj [Internet]. Elsevier B.V.; 2014;1840(6):1837. Available from: http://linkinghub.elsevier.com/retrieve/pii/S0304416514000403

53. Corriden R, Insel PA. Basal release of ATP: An autocrine-paracrine mechanism for cell regulation. Sci Signal. 2010;3(104).
54. Sluyter R, Shemon AN, Barden JA, Wiley JS. Extracellular ATP increases cation fluxes in human erythrocytes by activation of the P2X 7 receptor. J Biol Chem. 2004;279(43):44749–55.
55. Burnstock G. Blood cells: an historical account of the roles of purinergic signalling. Purinergic Signal. 2015;11(4):411–34.
56. Huber SM, Uhlemann A-C, Gamper NL, Duranton C, Kremsner PG, Lang F. Plasmodium falciparum activates endogenous Cl(-) channels of human erythrocytes by membrane oxidation. EMBO J [Internet]. 2002 Jan 15 [cited 2015 Dec 16];21(1–2):22–30. Available from: http://www.pubmedcentral.nih.gov/articlerender.fcgi?artid=125814&tool=pmcentrez&rendertype=abstract
57. Stringa PL, Romanin D, Lausada N, Papa Gobbi R, Zanuzzi C, Martín P, et al. Gut Permeability and Glucose Absorption Are Affected at Early Stages of Graft Rejection in a Small Bowel Transplant Rat Model. Transplant Direct [Internet]. 2017 Nov [cited 2018 Jun 25];3(11):e220. Available from: https://www.ncbi.nlm.nih.gov/pmc/articles/PMC5682765/pdf/txd-3-e220.pdf
58. Lillie R. Histopathologic technic and practical histochemistry. 1947 [cited 2018 Jun 8]; Available from: http://krishikosh.egranth.ac.in/bitstream/1/23040/1/IVRI OB 1826.pdf
59. Baker RF, Clark LJ. Assay of red cell membrane deformability with some applications. Biomed Biochim Acta [Internet]. 1983 [cited 2018 Jun 14];42(11–12):S91-6. Available from: http://www.ncbi.nlm.nih.gov/pubmed/6675722
60. Skals M, Jensen UB, Ousingsawat J, Kunzelmann K, Leipziger J, Praetorius HA. Escherichia coli alpha-hemolysin triggers shrinkage of erythrocytes via K(Ca)3.1 and TMEM16A channels with subsequent phosphatidylserine exposure. J Biol Chem [Internet]. 2010 May 14 [cited 2015 Dec 16];285(20):15557–65. Available from: http://www.jbc.org/content/285/20/15557.short
61. Bencic DC, Yates TJ, Ingermann RL. Ecto-ATPase activity of vertebrate blood cells. Physiol Zool. 1997;70(6):621–30.
62. Zimmermann H, Zebisch M, Sträter N. Cellular function and molecular structure of ecto-nucleotidases. Purinergic Signal. 2012;8(3):437–502.
63. Yegutkin GG. Enzymes involved in metabolism of extracellular nucleotides and nucleosides: Functional implications and measurement of activities. Crit Rev Biochem Mol Biol. 2014;49(6):473–97.
64. Lüthje J, Schomburg a, Ogilvie a. Demonstration of a novel ecto-enzyme on human erythrocytes, capable of degrading ADP and of inhibiting ADP-induced platelet aggregation. Eur J Biochem. 1988;175(2):285–9.
65. Yegutkin GG, Samburski SS, Jalkanen S. Soluble purine-converting enzymes circulate in human blood and regulate extracellular ATP level via counteracting pyrophosphatase and phosphotransfer reactions. FASEB J. 2003;17(10):1328–30.
66. Herlax V, Bakás L. Fatty acids covalently bound to α-hemolysin of Escherichia coli are involved in the molten globule conformation: Implication of disordered regions in binding promiscuity. Biochemistry. 2007;46(17):5177–84.
67. Lang E, Lang F. Mechanisms and pathophysiological significance of eryptosis, the suicidal erythrocyte death. Semin Cell Dev Biol [Internet]. Elsevier Ltd; 2015;39:35–42. Available from: http://dx.doi.org/10.1016/j.semcdb.2015.01.009
68. Herlax V, Maté S, Rimoldi O, Bakás L. Relevance of fatty acid covalently bound to Escherichia coli alpha-hemolysin and membrane microdomains in the oligomerization process. J Biol Chem [Internet]. American Society for Biochemistry and Molecular Biology; 2009 Sep 11 [cited 2017 Jun 26];284(37):25199–210. Available from: http://www.ncbi.nlm.nih.gov/pubmed/19596862

69. Munksgaard PS, Vorup-Jensen T, Reinholdt J, Söderström CM, Poulsen K, Leipziger J, et al. Leukotoxin from Aggregatibacter actinomycetemcomitans causes shrinkage and P2X receptor-dependent lysis of human erythrocytes. Cell Microbiol. 2012;14(12):1904–20.
70. Maté SM, Vázquez RF, Herlax VS, Daza Millone MA, Fanani ML, Maggio B, et al. Boundary region between coexisting lipid phases as initial binding sites for Escherichia coli alpha-hemolysin: a real-time study. Biochim Biophys Acta [Internet]. 2014 Jul [cited 2015 Dec 16];1838(7):1832–41. Available from: http://www.ncbi.nlm.nih.gov/pubmed/24613790
71. Ostolaza H, Bartolomé B, de Zárate IO, de la Cruz F, Goñi FM. Release of lipid vesicle contents by the bacterial protein toxin α-haemolysin. Biochim Biophys Acta - Biomembr [Internet]. Elsevier; 1993 Apr 8 [cited 2018 Jun 25];1147(1):81–8. Available from: https://www.sciencedirect.com/science/article/pii/000527369390318T?via%3Dihub
72. Morova J, Osicka R, Masin J, Sebo P. RTX cytotoxins recognize β2 integrin receptors through N-linked oligosaccharides. [cited 2018 Jun 14]; Available from: https://www.ncbi.nlm.nih.gov/pmc/articles/PMC2291121/pdf/zpq5355.pdf
73. Locovei S, Bao LL, Dahl G. Pannexin 1 in erythrocytes: Function without a gap. Proc Natl Acad Sci [Internet]. 2006 May 16 [cited 2015 Aug 1];103(20):7655–9. Available from: http://www.pnas.org/content/103/20/7655.full
74. Silverman WR, de Rivero Vaccari JP, Locovei S, Qiu F, Carlsson SK, Scemes E, et al. The pannexin 1 channel activates the inflammasome in neurons and astrocytes. J Biol Chem [Internet]. 2009 Jul 3 [cited 2015 Aug 1];284(27):18143–51. Available from: http://www.jbc.org/content/early/2009/05/04/jbc.M109.004804.abstract
75. Michalski K, Kawate T. Carbenoxolone inhibits Pannexin1 channels through interactions in the first extracellular loop. J Gen Physiol [Internet]. 2016;147(2):165–74. Available from: http://www.jgp.org/lookup/doi/10.1085/jgp.201511505
76. Sridharan M, Adderley SP, Bowles EA, Egan TM, Stephenson AH, Ellsworth ML, et al. Pannexin 1 is the conduit for low oxygen tension-induced ATP release from human erythrocytes. AJP Hear Circ Physiol [Internet]. 2010 Oct 1 [cited 2015 Aug 1];299(4):H1146–52. Available from: http://ajpheart.physiology.org/content/299/4/H1146.short
77. Qiu F, Wang J, Spray DC, Scemes E, Dahl G. Two non-vesicular ATP release pathways in the mouse erythrocyte membrane. FEBS Lett [Internet]. Federation of European Biochemical Societies; 2011 Nov 4 [cited 2015 Aug 7];585(21):3430–5. Available from: http://dx.doi.org/10.1016/j.febslet.2011.09.033
78. Sluyter R, Stokes L. Significance of P2X7 receptor variants to human health and disease. Recent Pat DNA Gene Seq. 2011;5(1):41–54.
79. Zimmermann H. Extracellular ATP and other nucleotides—ubiquitous triggers of intercellular messenger release. Purinergic Signal. 2016;12(1):25–57.
80. Leal Denis et al. 2016. PLoS One [Internet]. 2016; Available from: ournals.plos.org/plosone/article/authors?id=10.1371/journal.pone.0158305
81. De Backer D, Donadello K, Taccone FS, Ospina-Tascon G, Salgado D, Vincent J-L. Microcirculatory alterations: potential mechanisms and implications for therapy [Internet]. Annals of Intensive Care. 2011 [cited 2018 Sep 29]. Available from: http://www.annalsofintensivecare.com/content/1/1/27
82. Leal Denis M, Lauri N, Alvarez C, Lefevre S, Gonzalez-Lebrero R, Espelt M, et al. Effects of α-hemolysin on human erythrocytes. Part 1. Regulation of extracellular ATP and cell volume. Biochem J. 2018;
83. Burnstock G. Purinergic signalling: Its unpopular beginning, its acceptance and its exciting future. BioEssays. 2012;34(3):218–25.
84. Mempin R, Tran H, Chen C, Gong H, Kim Ho K, Lu S. Release of extracellular ATP by bacteria during growth. BMC Microbiol. 2013;13(1):1–13.

85. Alvarez CL, Corradi G, Lauri N, Marginedas-Freixa I, Leal Denis MF, Enrique N, et al. Dynamic regulation of extracellular ATP in *Escherichia coli*. Biochem J [Internet]. 2017;474(8):1395–416. Available from: http://biochemj.org/lookup/doi/10.1042/BCJ20160879
86. Lang F. Mechanisms and Significance of Cell Volume Regulation. J Am Coll Nutr. 2007;26(January 2015):613S–623S.
87. Manodori AB, Barabino GA, Lubin BH, Kuypers FA. Adherence of phosphatidylserine-exposing erythrocytes to endothelial matrix thrombospondin. Blood [Internet]. 2000 [cited 2017 Jun 23];95(4):1293–300. Available from: http://www.bloodjournal.org/content/95/4/1293.long?sso-checked=true
88. Hardeman MR, Dobbe JG, Ince C. The Laser-assisted Optical Rotational Cell Analyzer (LORCA) as red blood cell aggregometer. Clin Hemorheol Microcirc [Internet]. 2001 [cited 2018 Jun 14];25(1):1–11. Available from: http://www.ncbi.nlm.nih.gov/pubmed/11790865
89. Silva-Herdade AS, Freitas T, Almeida JP, Saldanha C. Erythrocyte deformability and nitric oxide mobilization under pannexin-1 and PKC dependence. Clin Hemorheol Microcirc [Internet]. 2015 [cited 2018 Jun 14];59(2):155–62. Available from: http://www.ncbi.nlm.nih.gov/pubmed/24595130

Highlights

- α-hemolysin induces ATP release by lytic and non-lytic mechanisms.
- α-hemolysin requires interaction with membrane proteins to induce ATP release.
- α-hemolysin induces reciprocal regulation of cell volume and ATP release, mediated by P2X receptors
- α-hemolysin induces lytic and non-lytic ATP release of erythrocytes perfussed through a mesentery.
- α-hemolysin induces shrinkage followed by irreversible swelling and high adhesivity of erythrocytes to endotelial cells.

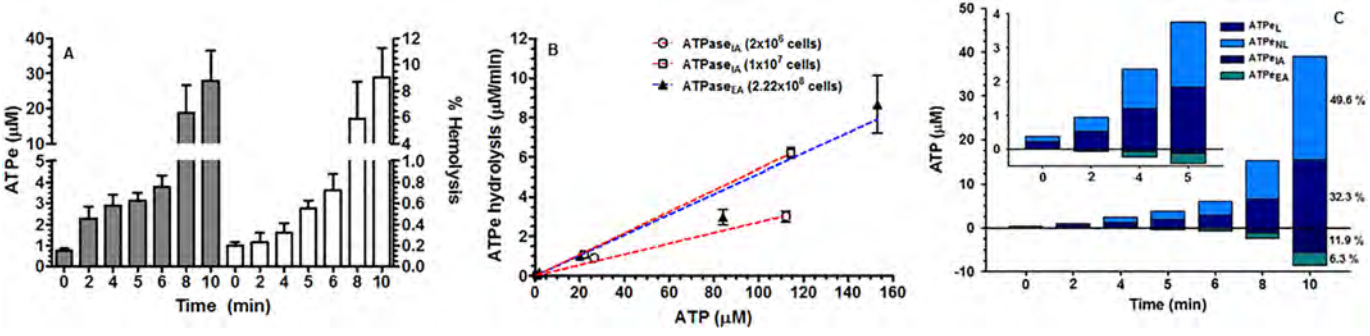
A
ATPe (μM)
% Hemolysis
Time (min)
B
ATPase$_{IA}$ (2x10^5 cells)
ATPase$_{IA}$ (1x10^7 cells)
ATPase$_{EA}$ (2.22x10^8 cells)
ATPe hydrolysis (μM/min)
ATP (μM)
C
ATPe$_L$
ATPe$_{NL}$
ATPe$_{IA}$
ATPe$_{EA}$
49.6 %
32.3 %
11.9 %
6.3 %
ATP (μM)
Time (min)

Figure 1

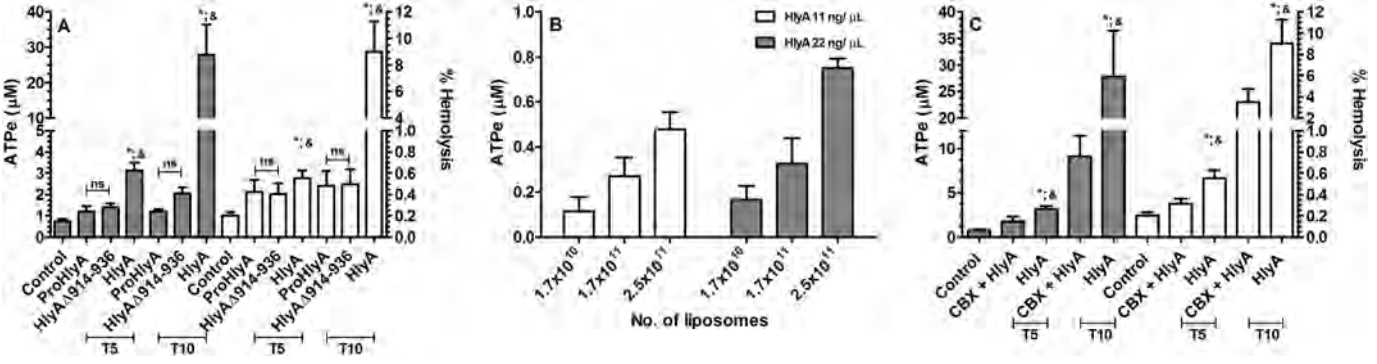
A
ATPe (μM)
% Hemolysis
ns
*;&
Control
ProHlyA
HlyAΔ914-936
HlyA
T5
T10
B
HlyA 11 ng/ μL
HlyA 22 ng/ μL
ATPe (μM)
1.7x10^10
1.7x10^11
2.5x10^11
No. of liposomes
C
ATPe (μM)
% Hemolysis
Control
CBX + HlyA
HlyA
T5
T10

Figure 2

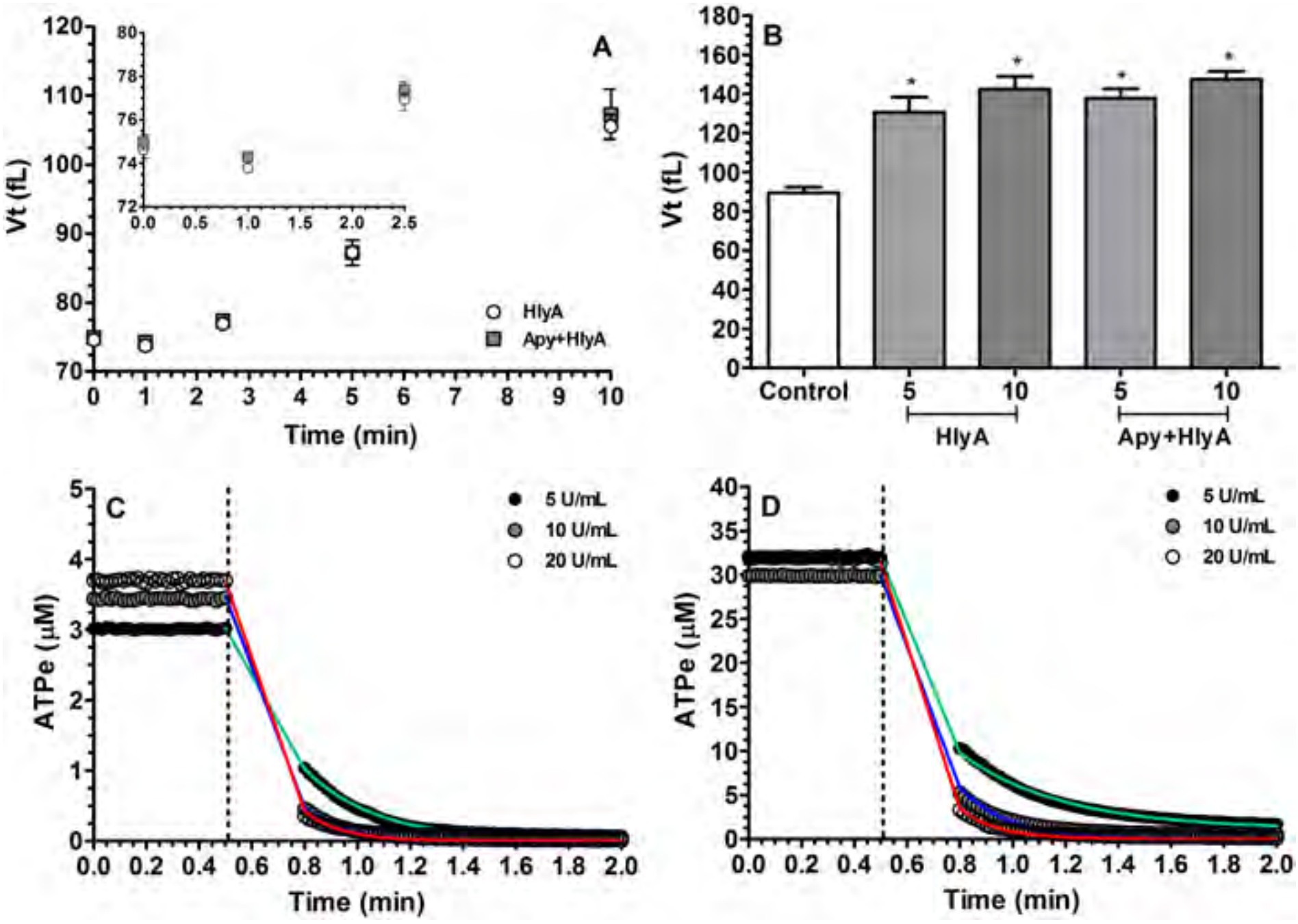
A
Vt (fL)
Time (min)
HlyA
Apy+HlyA
B
Vt (fL)
Control
5
10
5
10
HlyA
Apy+HlyA
C
ATPe (μM)
Time (min)
5 U/mL
10 U/mL
20 U/mL
D
ATPe (μM)
Time (min)
5 U/mL
10 U/mL
20 U/mL

Figure 3

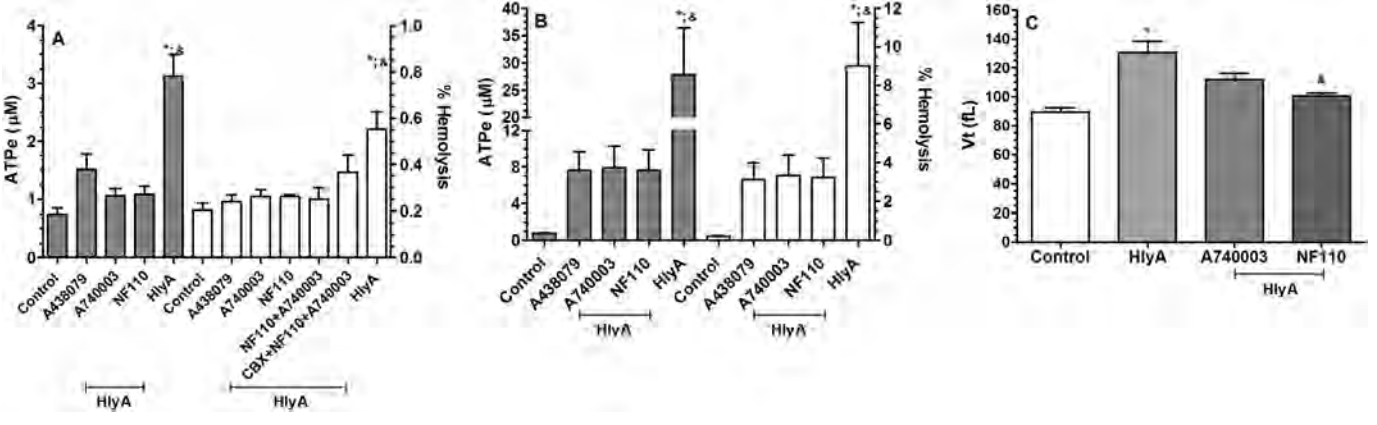
A
ATPe (μM)
% Hemolysis
Control
A438079
A740003
NF110
HlyA
NF110+A740003
CBX+NF110+A740003
HlyA
HlyA
B
ATPe (μM)
% Hemolysis
Control
A438079
A740003
NF110
HlyA
HlyA
HlyA
C
Vt (fL)
Control
HlyA
A740003
NF110
HlyA

Figure 4

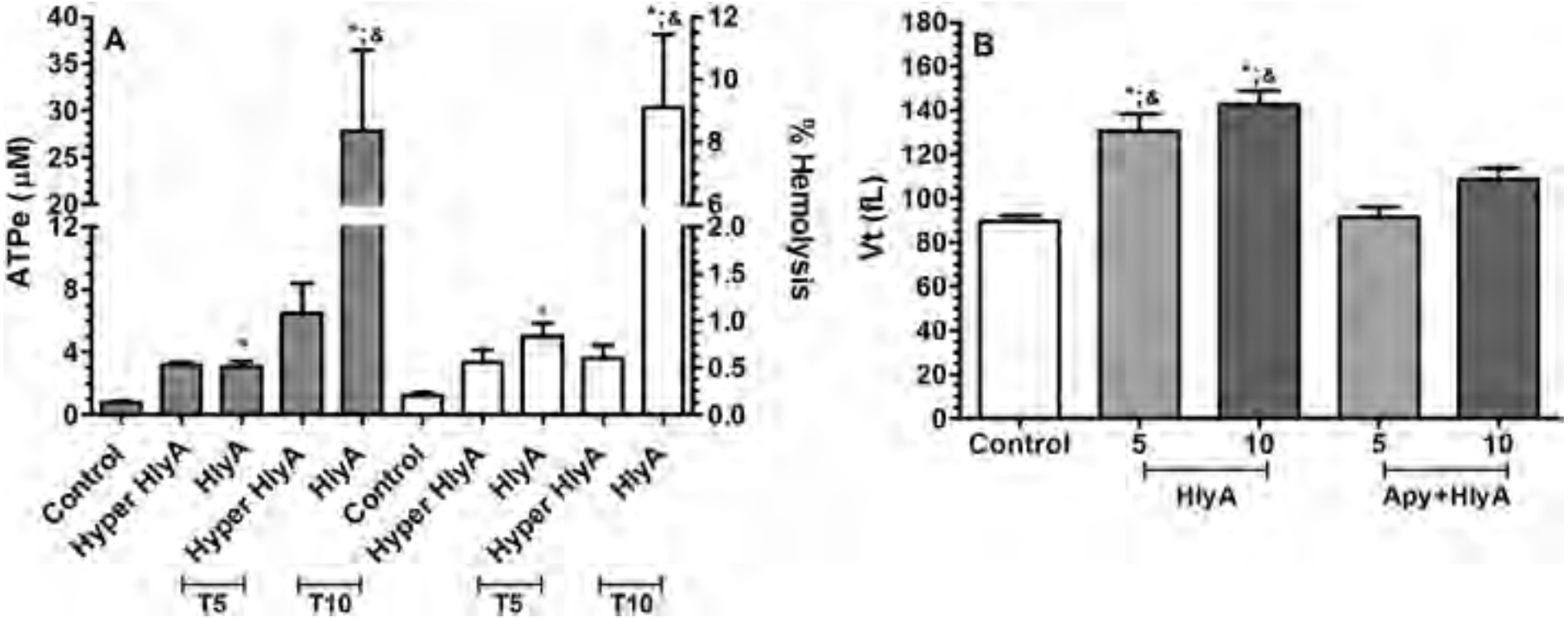
A
ATPe (μM)
% Hemolysis
Control
Hyper HlyA
HlyA
T5
T10
B
Vt (fL)
Control
5
10
HlyA
Apy+HlyA

Figure 5

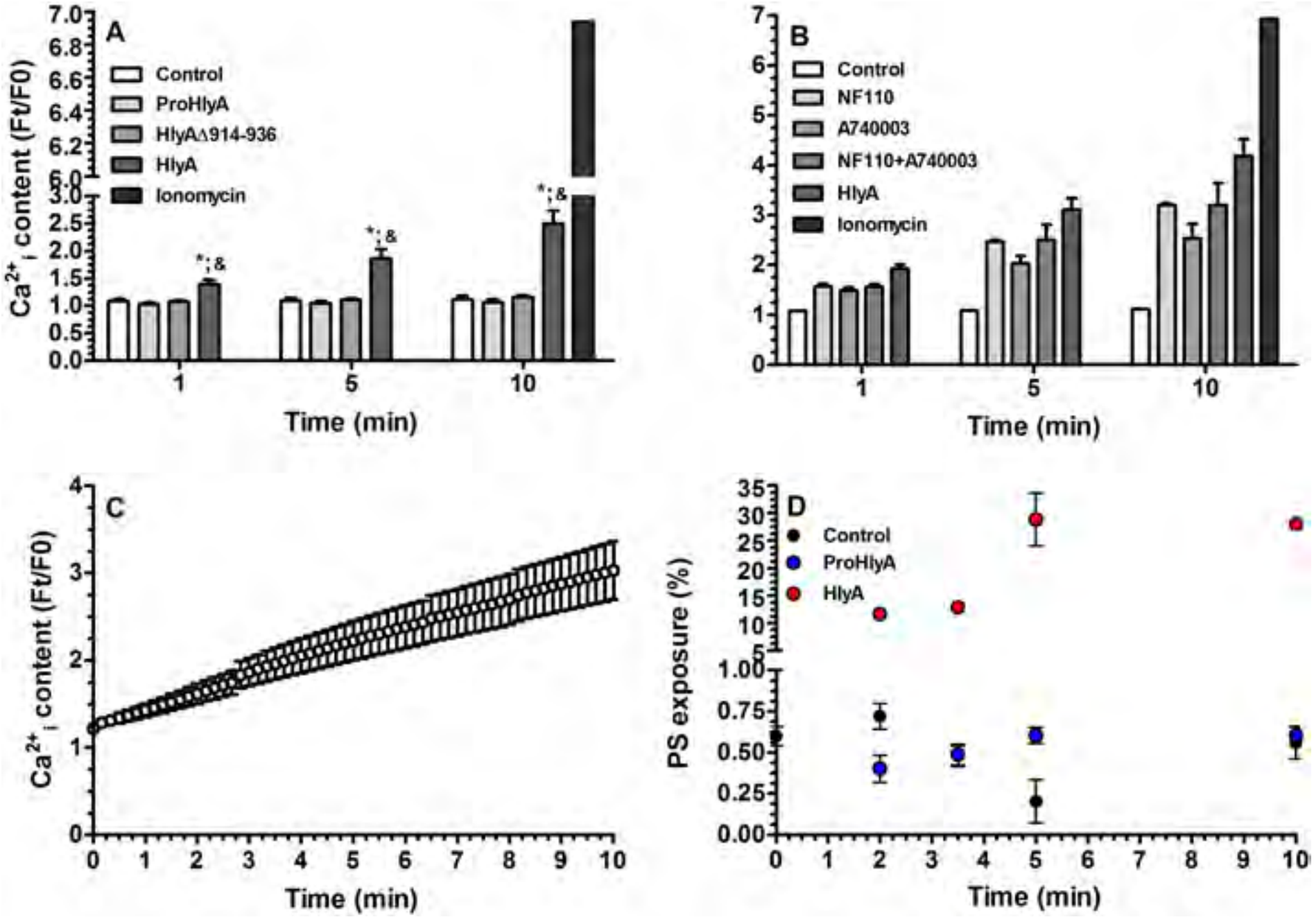
A
Control
ProHlyA
HlyAΔ914-936
HlyA
Ionomycin
$Ca^{2+}{}_i$ content (Ft/F0)
Time (min)
B
Control
NF110
A740003
NF110+A740003
HlyA
Ionomycin
Time (min)
C
$Ca^{2+}{}_i$ content (Ft/F0)
Time (min)
D
Control
ProHlyA
HlyA
PS exposure (%)
Time (min)

Figure 6

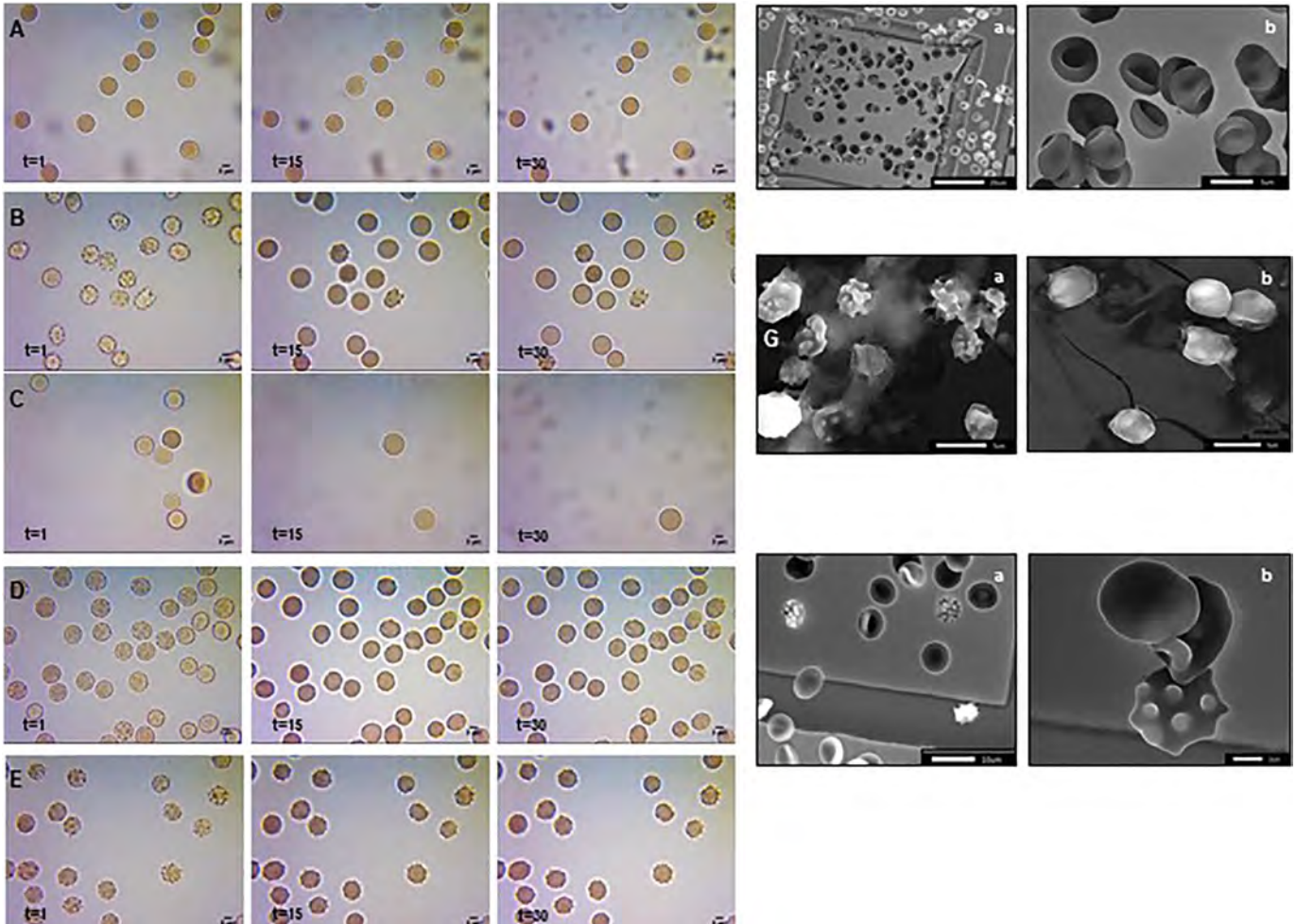
A
t=1
t=15
t=30
B
t=1
t=15
t=30
C
t=1
t=15
t=30
D
t=1
t=15
t=30
E
t=1
t=15
t=30
F
a
b
G
a
b
a
b

Figure 7

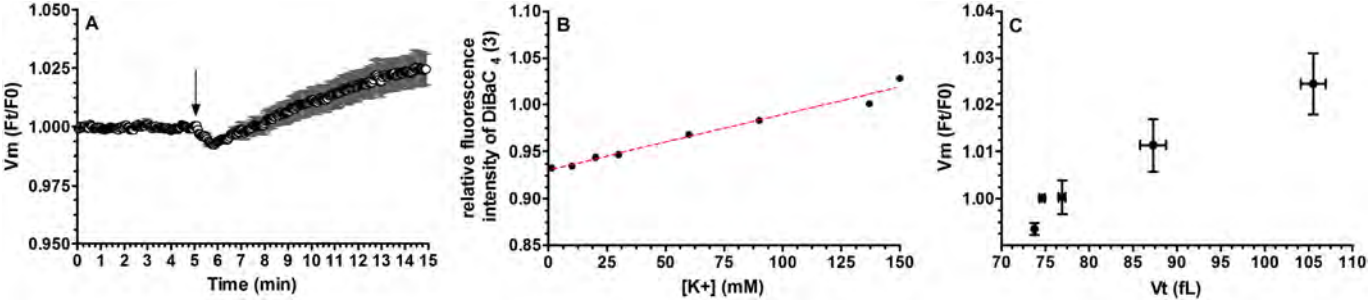
A
Vm (Ft/F0)
Time (min)
B
relative fluorescence intensity of DiBaC 4 (3)
[K+] (mM)
C
Vm (Ft/F0)
Vt (fL)

Figure 8

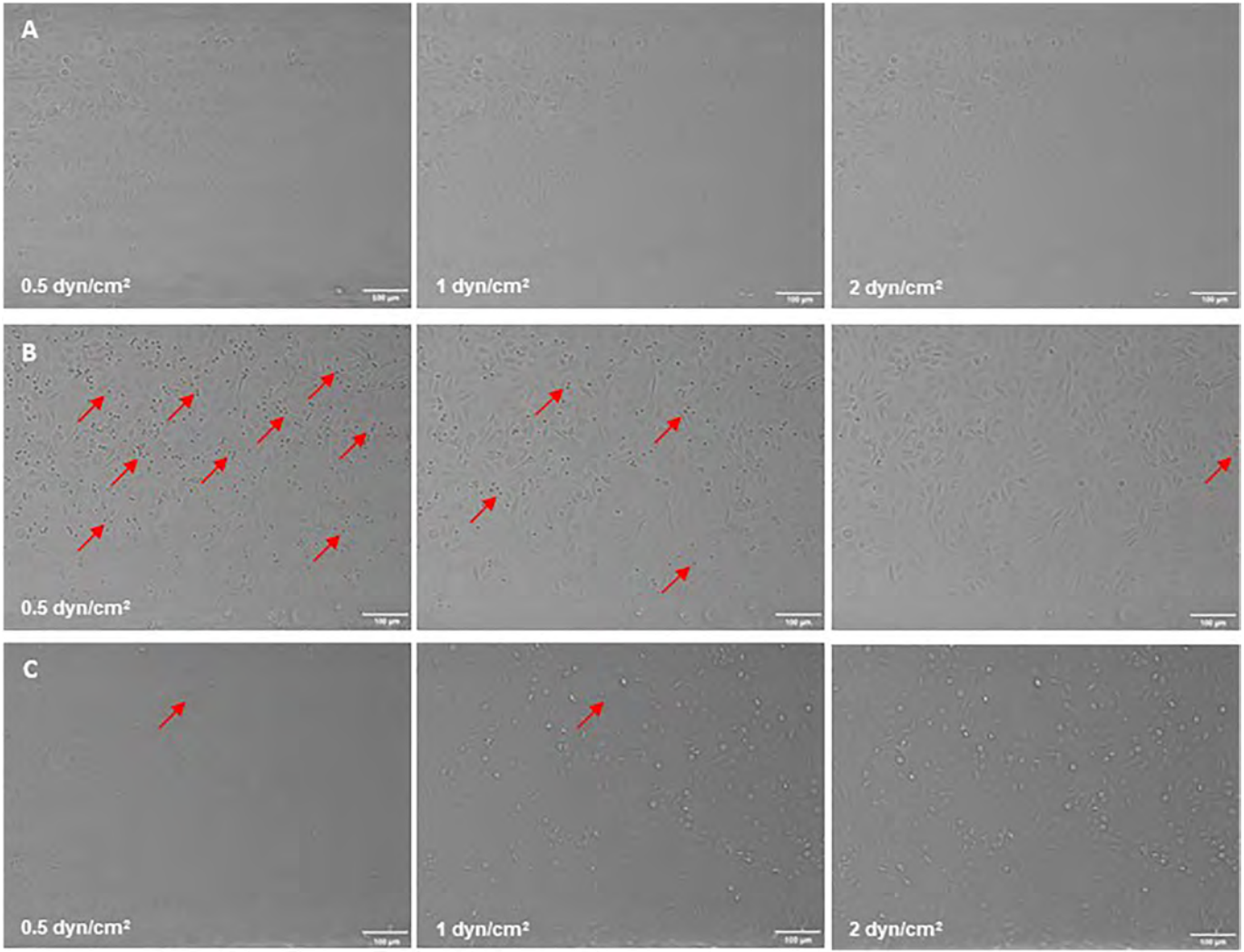
A
0.5 dyn/cm²
1 dyn/cm²
2 dyn/cm²
B
0.5 dyn/cm²
C
0.5 dyn/cm²
1 dyn/cm²
2 dyn/cm²

Figure 9

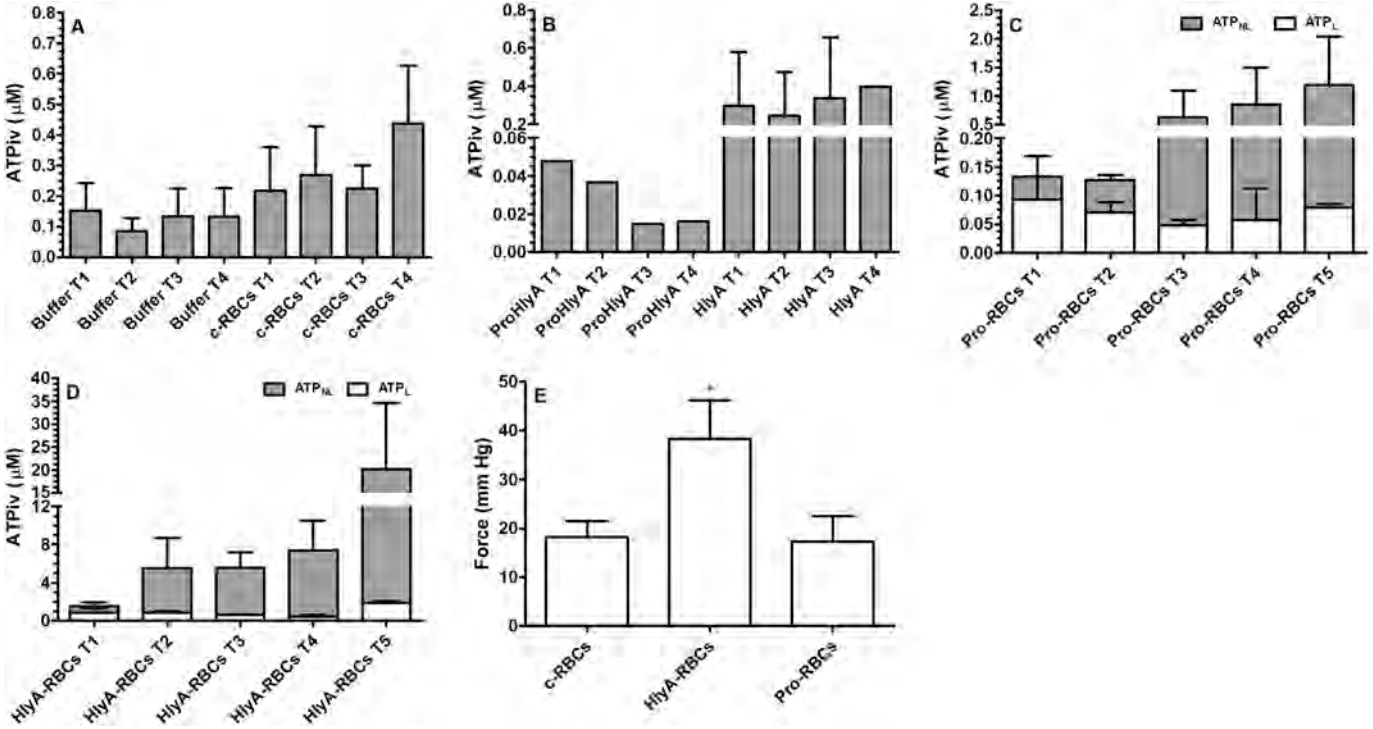
A
ATPiv (μM)
Buffer T1
Buffer T2
Buffer T3
Buffer T4
c-RBCs T1
c-RBCs T2
c-RBCs T3
c-RBCs T4
B
ATPiv (μM)
ProHlyA T1
ProHlyA T2
ProHlyA T3
ProHlyA T4
HlyA T1
HlyA T2
HlyA T3
HlyA T4
C
ATPNL
ATPL
ATPiv (μM)
Pro-RBCs T1
Pro-RBCs T2
Pro-RBCs T3
Pro-RBCs T4
Pro-RBCs T5
D
ATPNL
ATPL
ATPiv (μM)
HlyA-RBCs T1
HlyA-RBCs T2
HlyA-RBCs T3
HlyA-RBCs T4
HlyA-RBCs T5
E
Force (mm Hg)
c-RBCs
HlyA-RBCs
Pro-RBCs

Figure 10

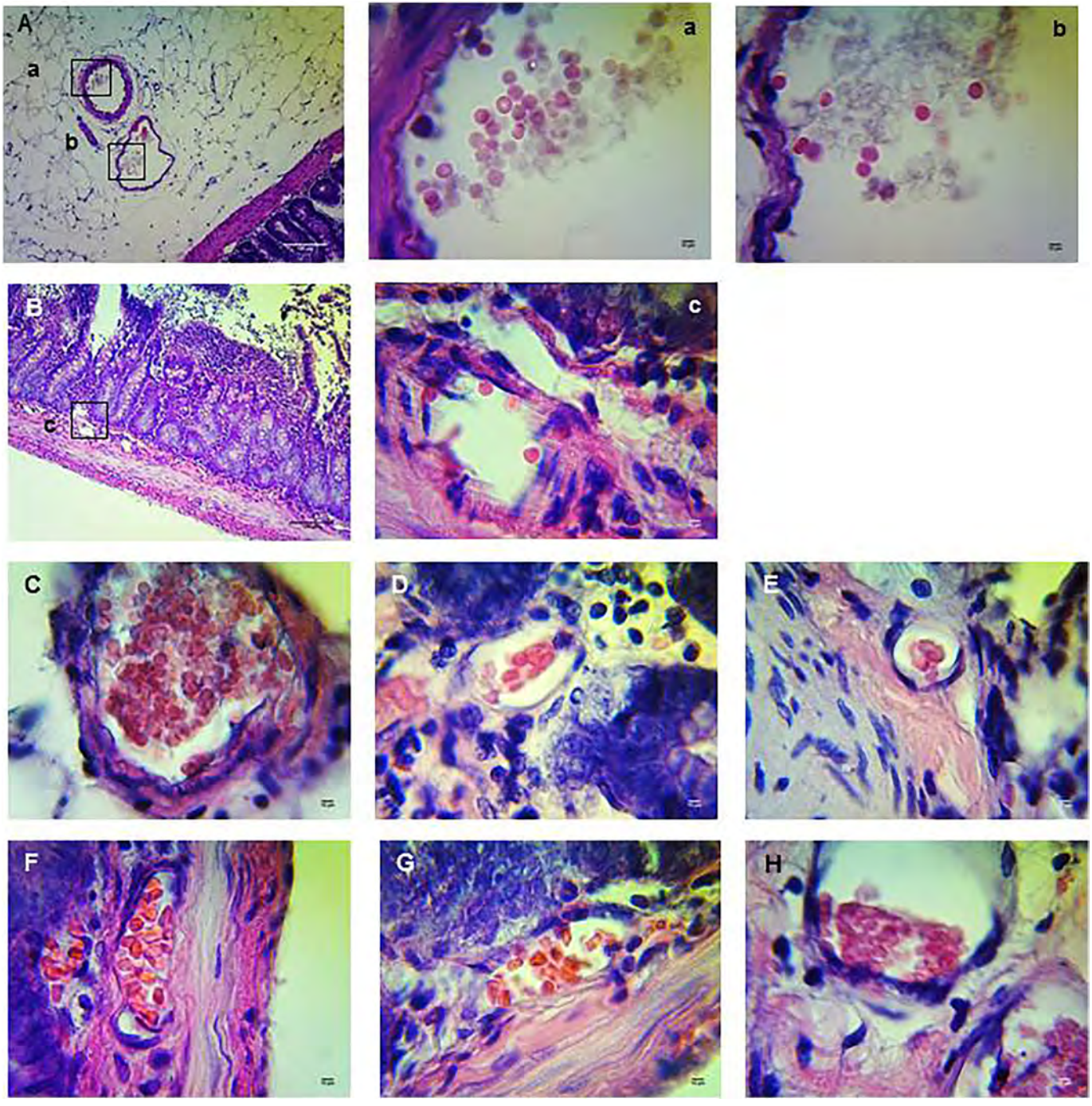

Figure 11

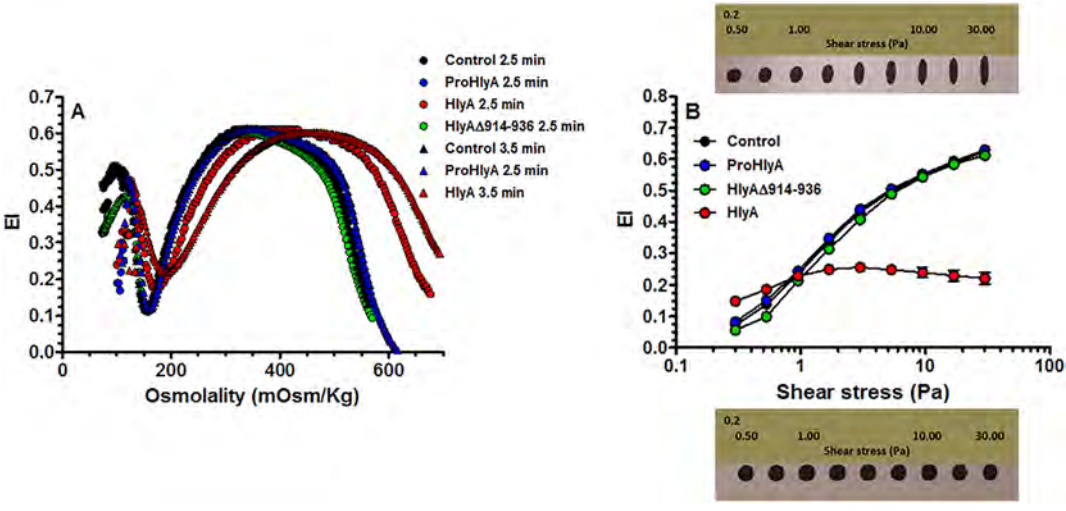
A
EI
Osmolality (mOsm/Kg)
Control 2.5 min
ProHlyA 2.5 min
HlyA 2.5 min
HlyAΔ914-936 2.5 min
Control 3.5 min
ProHlyA 2.5 min
HlyA 3.5 min
B
EI
Shear stress (Pa)
Control
ProHlyA
HlyAΔ914-936
HlyA
0.2
0.50
1.00
10.00
30.00
Shear stress (Pa)

Figure 12

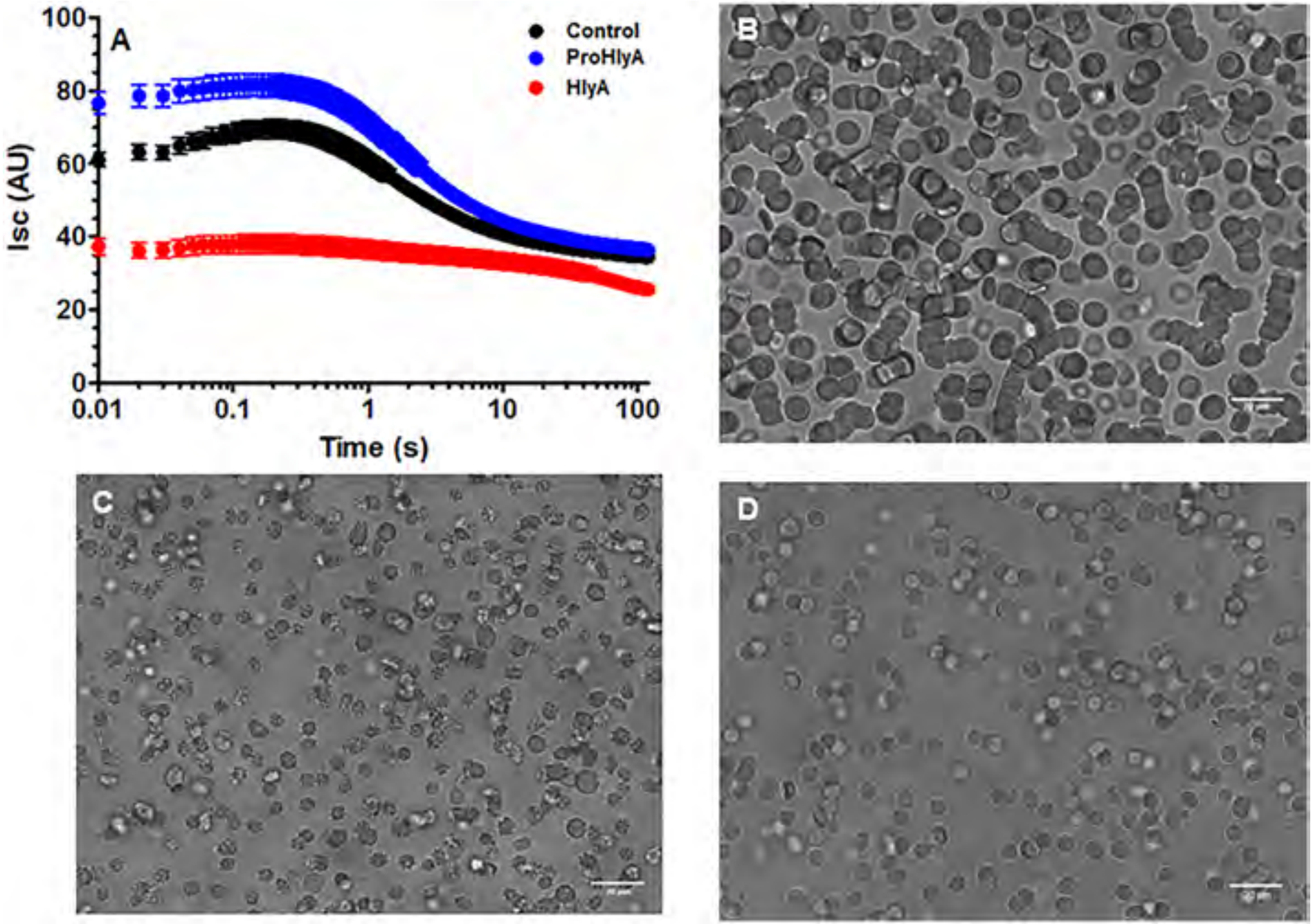
A
Control
ProHlyA
HlyA
Isc (AU)
100
80
60
40
20
0
0.01
0.1
1
10
100
Time (s)
B
C
D

Figure 13

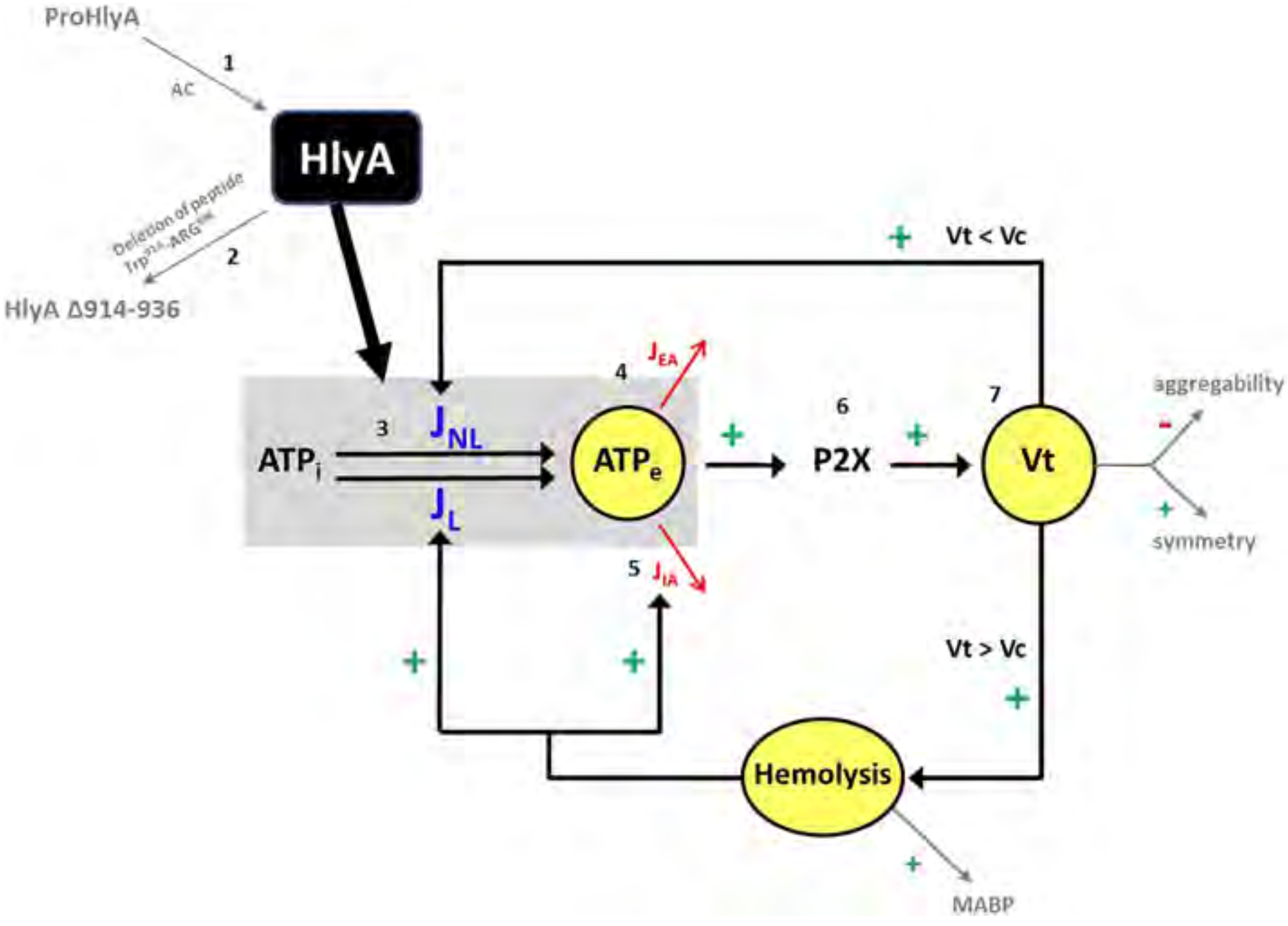
ProHlyA
1
AC
HlyA
Deletion of peptide
2
HlyA Δ914-936
+ Vt < Vc
4
J_{EA}
3
J_{NL}
ATP_i
ATP_e
J_L
5 J_{IA}
6
P2X
7
Vt
aggregability
-
+
symmetry
+
+
+
+
Vt > Vc
+
Hemolysis
+
MABP

Figure 14

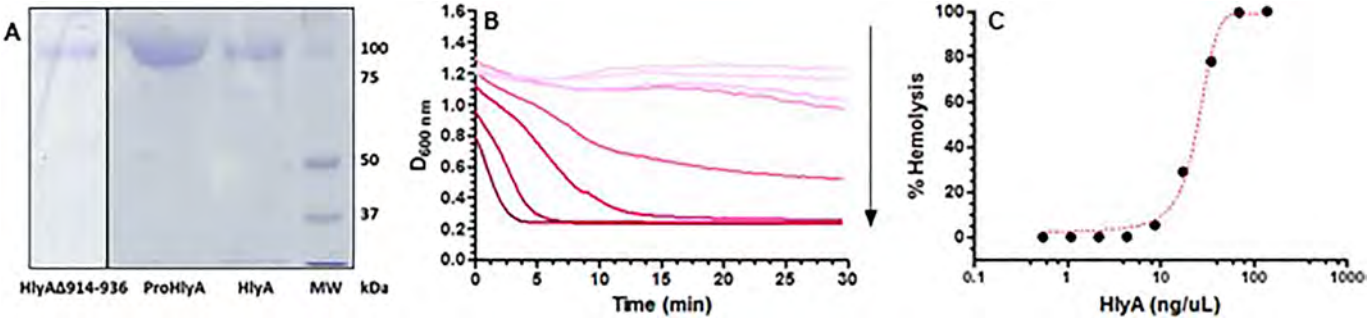
A
100
75
50
37
HlyAΔ914-936
ProHlyA
HlyA
MW
kDa
B
1.6
1.4
1.2
1.0
0.8
0.6
0.4
0.2
0.0
D600 nm
0
5
10
15
20
25
30
Time (min)
C
100
80
60
40
20
0
% Hemolysis
0.1
1
10
100
1000
HlyA (ng/uL)

Figure 15

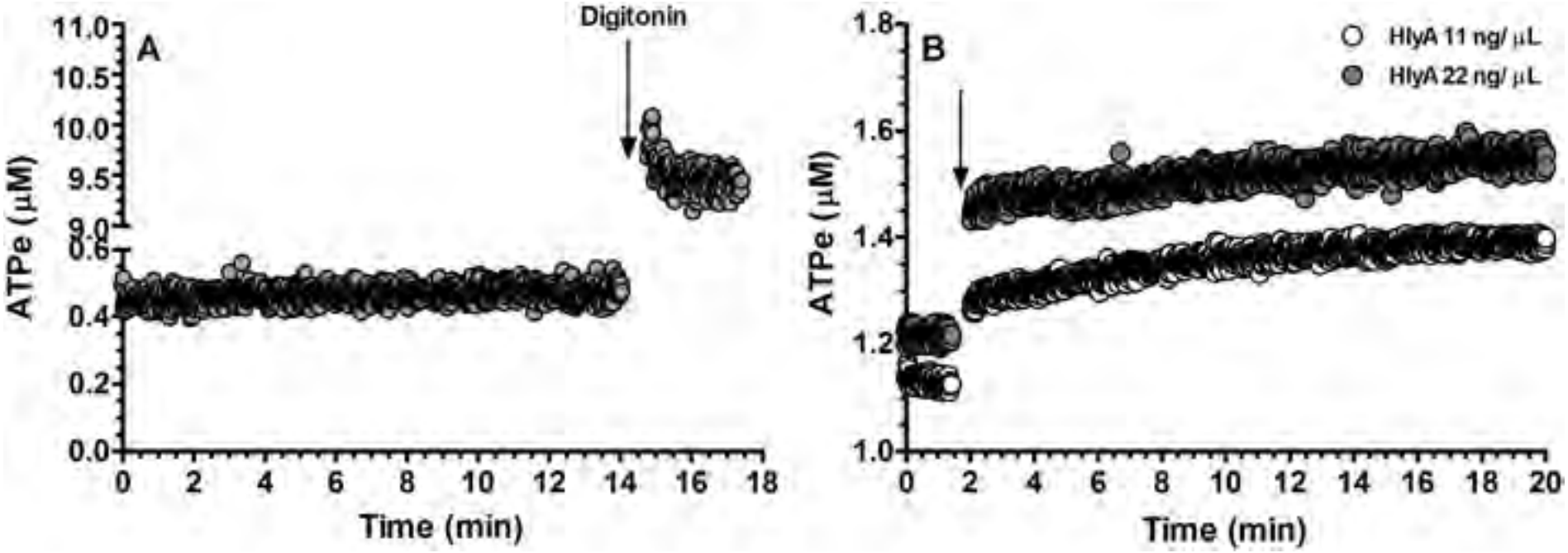
A
Digitonin
ATPe (μM)
Time (min)
B
HlyA 11 ng/ μL
HlyA 22 ng/ μL
ATPe (μM)
Time (min)

Figure 16

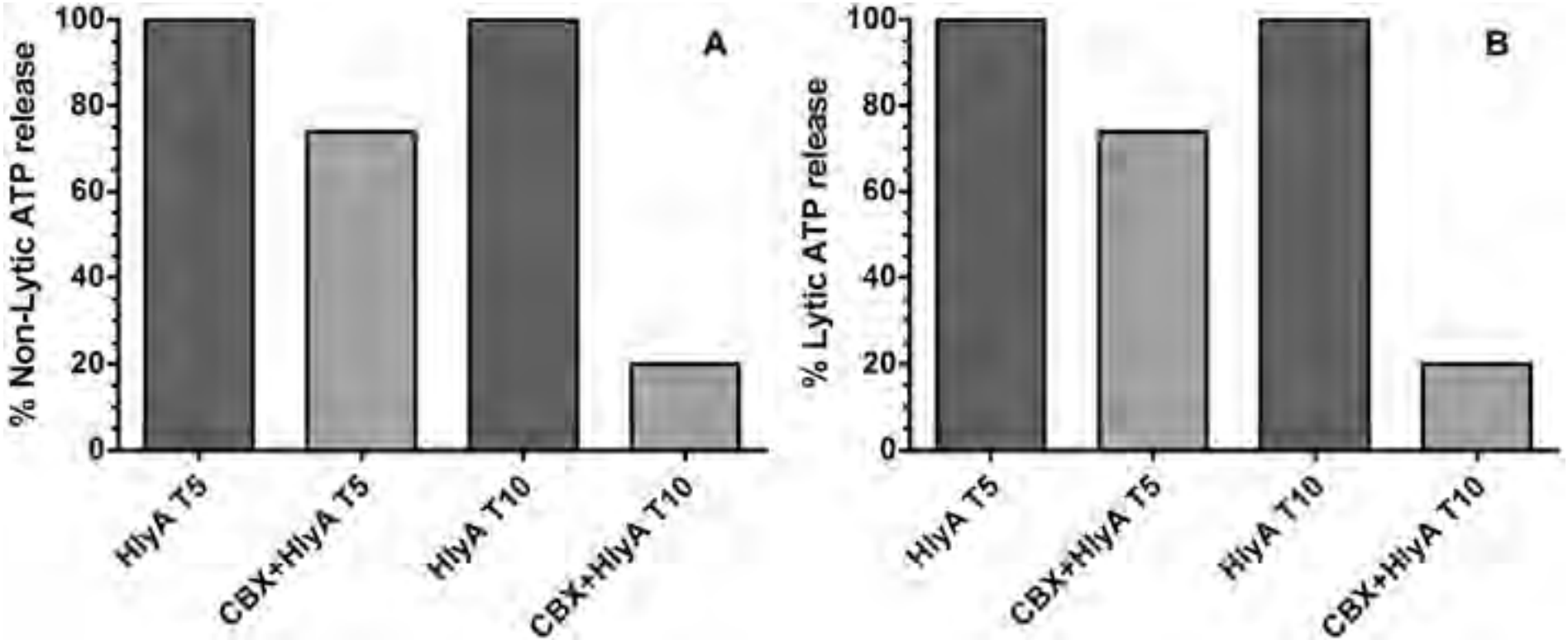
A
% Non-Lytic ATP release
100
80
60
40
20
0
HlyA T5
CBX+HlyA T5
HlyA T10
CBX+HlyA T10
B
% Lytic ATP release
100
80
60
40
20
0
HlyA T5
CBX+HlyA T5
HlyA T10
CBX+HlyA T10

Figure 17

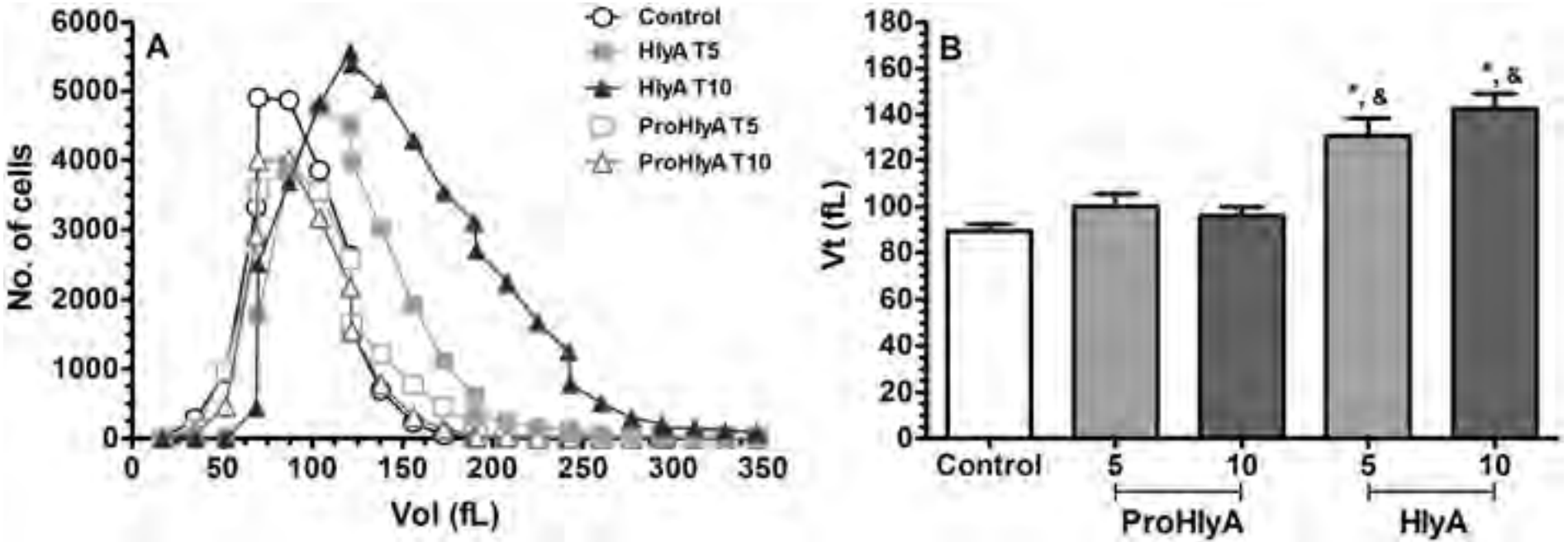
A
No. of cells
Vol (fL)
Control
HlyA T5
HlyA T10
ProHlyA T5
ProHlyA T10
B
Vt (fL)
Control
5
10
5
10
ProHlyA
HlyA
*, &
*, &

Figure 18

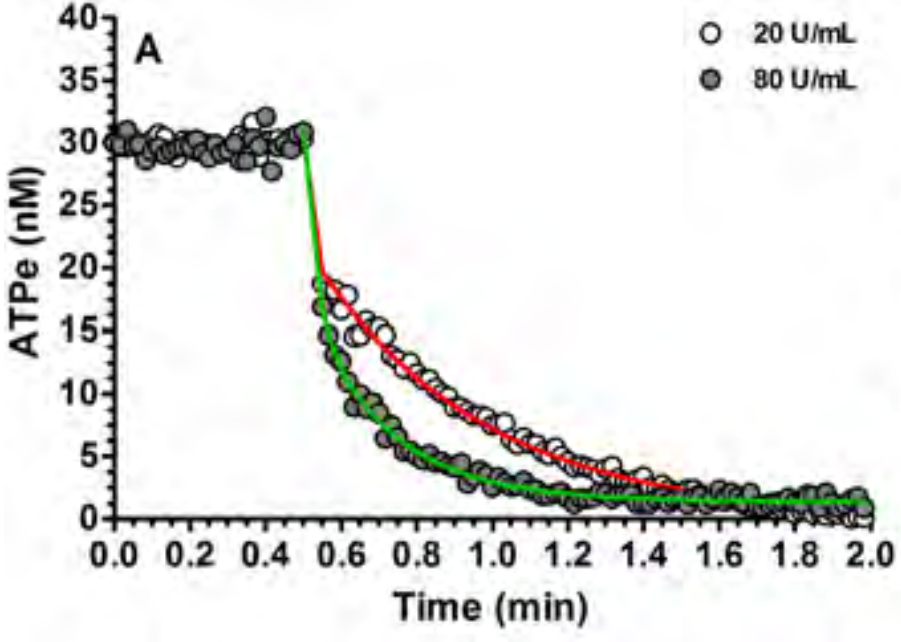
A
20 U/mL
80 U/mL
ATPe (nM)
Time (min)
0.0 0.2 0.4 0.6 0.8 1.0 1.2 1.4 1.6 1.8 2.0
0 5 10 15 20 25 30 35 40

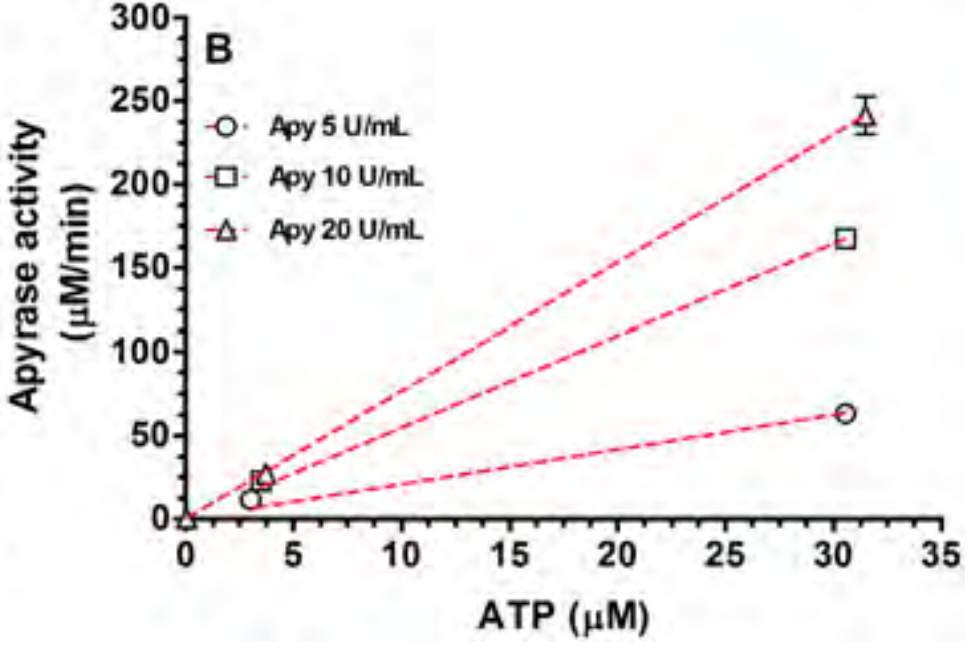
B
Apy 5 U/mL
Apy 10 U/mL
Apy 20 U/mL
Apyrase activity (µM/min)
ATP (µM)
0 5 10 15 20 25 30 35
0 50 100 150 200 250 300

Figure 19

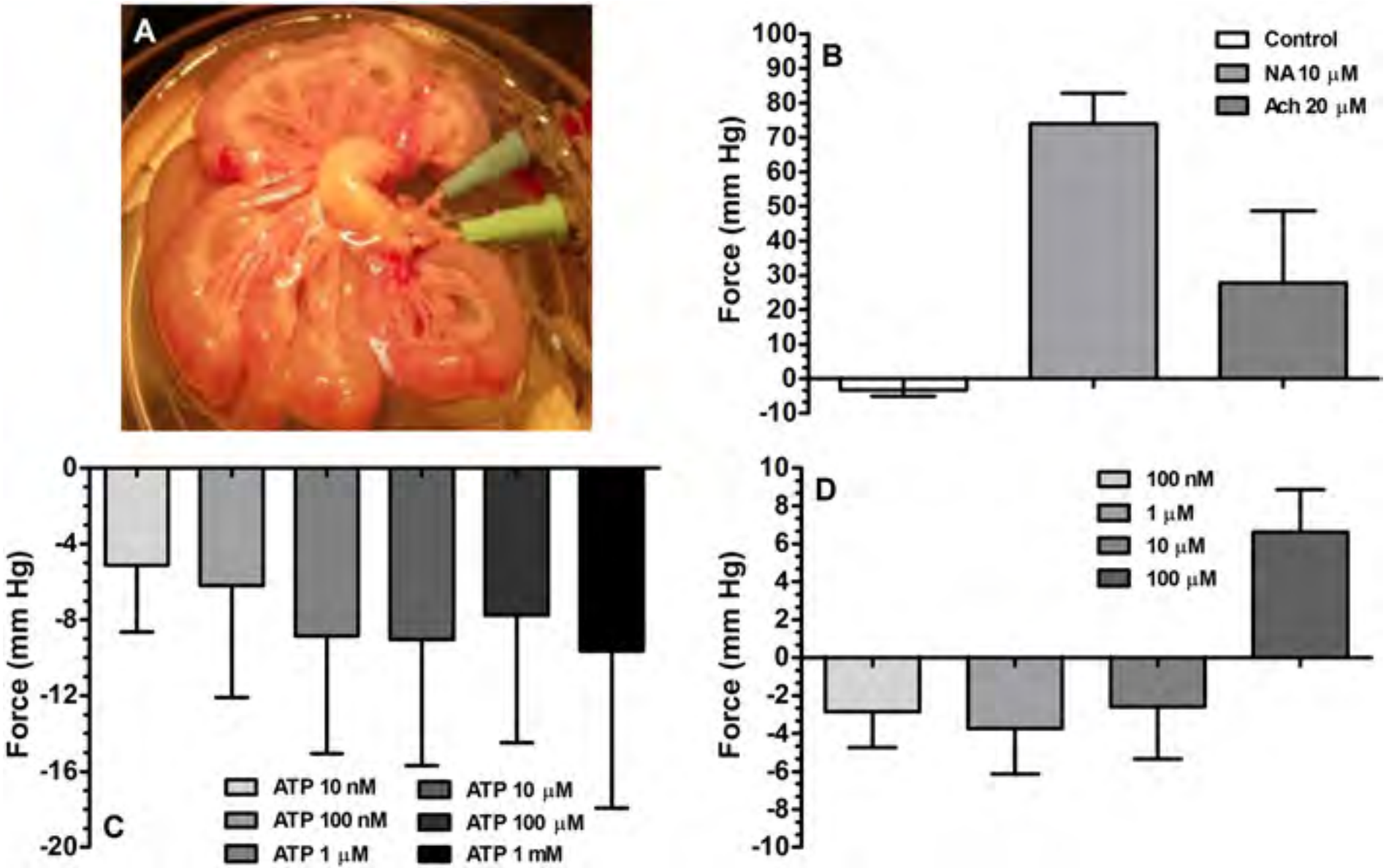
A
B
Force (mm Hg)
100
90
80
70
60
50
40
30
20
10
0
-10
Control
NA 10 μM
Ach 20 μM
C
Force (mm Hg)
0
-4
-8
-12
-16
-20
ATP 10 nM
ATP 100 nM
ATP 1 μM
ATP 10 μM
ATP 100 μM
ATP 1 mM
D
Force (mm Hg)
10
8
6
4
2
0
-2
-4
-6
-8
-10
100 nM
1 μM
10 μM
100 μM

Figure 20

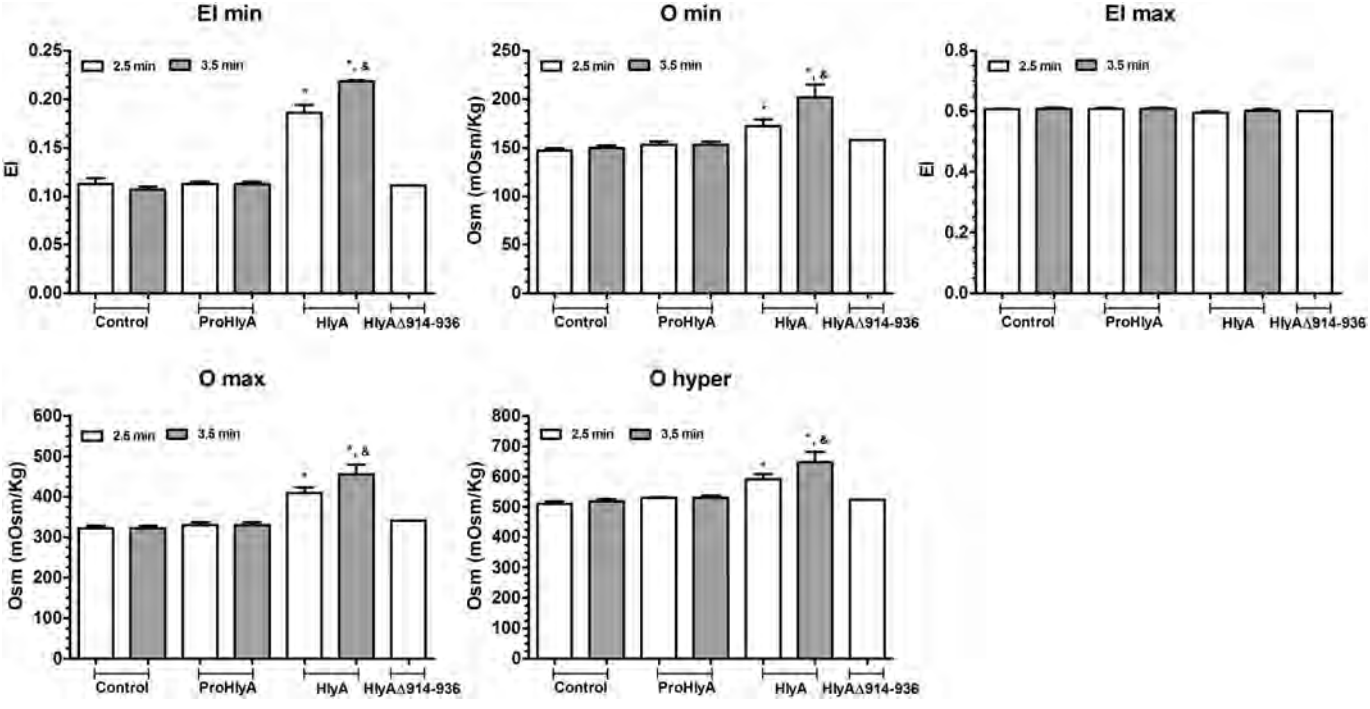
EI min
2.5 min
3.5 min
EI
0.25
0.20
0.15
0.10
0.05
0.00
Control
ProHlyA
HlyA
HlyAΔ914-936
O min
Osm (mOsm/Kg)
250
200
150
100
50
EI max
0.8
0.6
0.4
0.2
0.0
O max
600
500
400
300
200
100
0
O hyper
800
700
600
500
400
300
200
100

Figure 21